Thermal Output and Thermal Compensation Models for Apparent Strain in a Structural Health Monitoring-Based Environment

by

Enoch A–iyeh

A Thesis submitted to the Faculty of Graduate Studies of

The University of Manitoba

In Partial Fulfillment of the Requirements for the Degree of

Master of Science

Department of Electrical and Computer Engineering

University of Manitoba

Winnipeg, Manitoba

© Enoch A-iyeh, December 2012

Abstract

Structural Health Monitoring (SHM) is widely used to monitor the short and long-term behavior of intelligent structures. This monitoring can help prolong the useful service lives and identify deficiencies before possible damage of such structures.

The sensing systems that are usually deployed are intended to faithfully relay readings that reflect the true conditions of these structures. Unfortunately, this is seldom the case due to the presence of errors in the collected data.

The electrical strain gauges used in SHM environments for instrumentation purposes are susceptible to numerous sources of error. Apparent strain is known to be the most serious of all such errors. However or whichever way temperature variations of the gauge's environment occurs, apparent strain is introduced.

This work focuses on modeling apparent strain in an SHM environment using National Instruments' (NI) hard and software. The results of this work are applicable for thermal compensation in current test programs.

Acknowledgements

I sincerely acknowledge and appreciate the friendship and leadership of my supervisor Dr. Dean K. McNeill in this work. His genuine curiosity for answers to help save our bridges has inspired every aspect of this work.

The financial support of the Department of Innovation, Energy and Mines of the Province of Manitoba is greatly appreciated. It made the fiscal aspects of this project possible.

I am also grateful to the team in the McQuade Heavy Structures Laboratory for assistance in some experimental aspects of this work.

Last but not least, I acknowledge the love of God Almighty and my family. Thank you for all the little things, they mean a lot to me.

./Enoch

Dedication

I dedicate this work to the memory of my late mother–Veronica A-iyeh.

Contents

List of Figures

List of Tables

Chapter 1

Introduction and Problem Definition

1.1 Introduction

The need for "efficient and accurate measurement of quantities, such as voltage, current, strain, temperature, pressure, flow rate and force is of critical importance today and for the foreseeable future" [1]. This is necessary for accurate instrumentation of components. This is especially so in *structural health monitoring* (SHM), where numerous sources of error can obscure the precision of delicate strain measurements.

Strain is fundamental in engineering applications [3]. Wherever strain readings are desired, whether in an engine part or on the steel girder of a bridge, the answers to these questions are within our grasp [3]. Strain is common in objects that experience forces applied to them. Strain is defined as the ratio of change in dimension (ΔL) to the original dimension (L).

Presently, there is no direct scientific method of measuring stress in components and as a result, we resort to measuring the strain of the surface in order to know the internal stress of the material–an important factor because stress defines whether a part will bend or break. Strain gauges are among the most common transducers used to measure surface strain [3]. Mathematically, strain is expressed

$$\varepsilon = \Delta L / L \tag{1.1}$$

1.2 Problem Definition

The data outputs of strain gauges are relied upon for making major decisions as to the conditions of intelligent infrastructure such as bridges. It is therefore imperative to ensure that strain readings contain minimum or no errors by addressing all sources of error or to at least address the most influential of those errors.

The work reported in this thesis focuses on characterizing the most serious of such errors in an SHM application and developing models to compensate for them.

Chapter 2

Literature Review and State of the Art

There is little information in the literature dealing with obtaining accurate strain measurements with strain gauges and or correcting measurements for important errors [4]. This chapter mainly deals with strain gauge–Wheatstone bridge systems for strain measurements.

2.1 Types of Strain Gauges Used in Measurement Applications

Normally, strain gauges are categorized by their construction into five groups: Mechanical, optical, electrical, acoustical and pneumatic [1,2,3]. There are many types of strain gauges and among them is the universal foil strain gauge, which has a grid-shaped sensing element on the base of a thick plastic film and laminated within the film.

Strain gauges are manufactured from a wide variety of materials, the most common of which are constantan, isoelastic and copper-nickel alloys [13]. The most important properties of a gauge for any application are repeatability, stability, uniformity of gauge characteristics, etc.

A strain-sensing element may consist of either a length of very fine wire looped into a definite grid pattern to obtain the necessary length for a specific resistance value, or a grid that is photo-etched from a very thin sheet of metallic foil. Gauges constructed based on the former principle are called bonded-wire resistance gauges while those constructed based on the latter are called bonded-metal-foil strain gauges [3]. Below is a table of some gauge materials, their compositions, gauge factors and specific resistance values.

Table 1. Stain gauge materials and properties

Name of alloy or material	Composition	Gauge Factor	Specific resistance (μΩm)
Nichrome V	Ni-80%,Cr-20%	+2.1	0.98
Manganin	Ni-4%,Mn-12%, Cu-84%	+0.47	N/A
Advance (Constantan)	Ni-45%,Cu-55%	+2.1	0.49
Copel	Ni-45%,Cu-55%	+2.4	N/A
Annealed Constantan	Ni-40%,Cu-60%	+2.1	0.49
Isoelastic	Ni-36%,Cr-8%,Fe-55.5%,Mo-0.5%	+3.6	1.12
Karma	Ni-74%,Cr-20%, Al-3%,Fe-3%	+2.0	1.35
Platinum-Tungsten	Pt-92%,W-8%	+4.0	N/A
Armour D	Fe-80%,Cr-20%, Al-20%	+2.0	N/A
Carbon	100% C	+20.0	N/A

Sources: [1,2,3].

2.2 Applications of Strain Gauges

The applications or uses of strain gauges are numerous and are in principle limited only by the imaginations of the user [3]. Here are some of the uses of strain gauges:

1. They are used in theoretical investigations for checking and verifying elasticity of objects;
2. Strain gauges are widely used to obtain general information which can lead

indirectly to superior designs;

3. Use has been made of strain gauges in studying stresses in bridge members and stresses at railroad-track curves;
4. They have been used in investigating stresses induced in ship plates during the launching process.

These are but a few of the possible and diverse uses of strain gauges. Whether they are used in SHM of bridges or elsewhere, errors are present in readings and therefore need attention.

This work focuses on bonded-wire resistance strain gauges used in the SHM of bridges and the characterization of their attendant errors in such situations so that readings maybe corrected.

2.3 Basic Instrumentation and Operation of Strain Gauges

The bonded wire resistance strain gauge operates on the principle that the electrical resistance of the gauge varies with strain. To make use of this fact, the gauge must be connected in some circuit for measuring small changes in electrical resistance [3]. These strain gauges are also characterized by their sensitivity to strain for instrumentation purposes.

The gauge factor or sensitivity (G) of the gauge is related to the resistance and length of the element as follows:

$$G = \frac{\Delta R/R}{\Delta L/L} = \frac{\Delta R/R}{\varepsilon} \tag{2.1}$$

Where:

ΔR: Change in resistance

R: Initial resistance

ΔL: Change in length of element

L: Original length of element

ε: Strain.

Thus, strain sensitivity is defined by the resistance change (ΔR) per unit of the initial resistance (R) per unit of the applied axial strain.

The magnitude of the resistance change in the gauge corresponding to a particular force on the test piece being investigated is the value of ΔR in equation 2.1 The values of R, the nominal resistance, and G, the gauge factor, are usually known because the strain gauge manufacturer supplies them.

The only unknown quantity left to be specified in the equation is $\Delta L/L$, the unit change in strain. Equation 2.1 can thus be written as

$$\varepsilon = \frac{\Delta L}{L} = \frac{\Delta R/R}{G} \tag{2.2}$$

In other words, unit strain is the ratio of unit change in resistance ($\Delta R/R$) to the gauge factor (G) [3].

This procedure is all very simple except for one thing–some device is needed for measuring ΔR adequately and accurately [3].

Conventional ohmmeters are not used in measuring the changes in resistance often

encountered in strain applications. This is due to the small nature of the changes in resistance There is a form of electrical circuits, which handle such situations adequately and are common in strain applications–bridge-type circuits. The Wheatstone bridge circuit is very commonly used for strain applications [3]. A circuit diagram of a Wheatstone bridge is shown in figure 1.

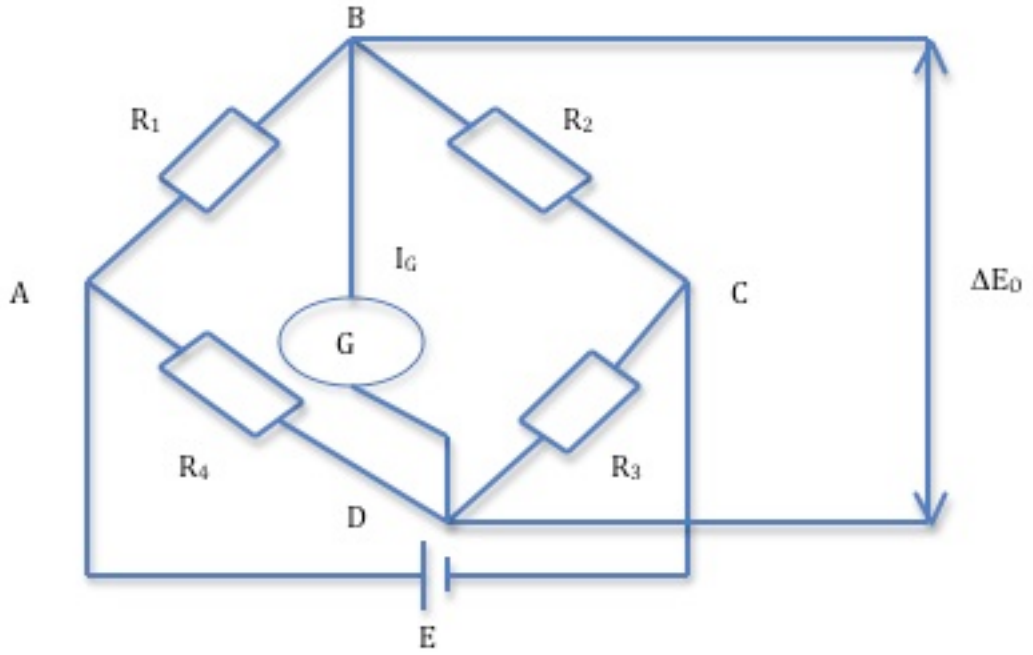

Fig. 1. A Wheatstone bridge circuit

The bridge circuit above is widely employed for precision measurement of resistance. The circuit is composed of four resistors connected in a definite pattern, a battery or a current source and a sensitive instrument e.g. a galvanometer. A galvanometer was not used in the Wheatstone bridges discussed in this work. The operation of the bridge is therefore discussed in terms of the current through arm BD, I_G and the output voltage across arm BD, ΔE_o. The output voltage, ΔE_o, in these situations is measured by an

analogue to digital converter. With the aid of the Wheatstone bridge, small changes in resistance are amplified and measured [3].

In Fig. 1 above, assume that the value of R_1 is unknown but the values of R_2, R_3 and R_4 are known precisely. It is known that the relation between the resistors when equilibrium prevails is

$$R_1 / R_4 = R_2 / R_3$$

$$R_1 R_3 = R_2 R_4 \tag{2.3}$$

From this relation, the value of the unknown resistance R_1 is computed as

$$R_1 = \left(R_2 / R_3 \right) R_4$$

Changes in the value of R_1 can be computed in a similar manner but with some modifications pertaining to the situation.

When the Wheatstone bridge is balanced, the ΔE_o is zero. However, a small change in resistance in any of the arms of the bridge would cause a non-zero current reading.

In practical applications, R_1 could serve as the resistance of the strain gauge (quarter bridge configuration).

After a strain gauge is cemented to a test piece and connected into the bridge as R_1, equilibrium can be established by adjusting the ratio R_2 / R_3, thus determining the exact resistance of the gauge that corresponds to zero or no load [3]. The appropriate and careful application of strain gauges can lead to understanding the behavior of structural members and machine parts under operating conditions [3].

The Wheatstone bridge circuit operates in two major modes. It may be in a balance mode

or it may be out of balance. The two operating conditions are described next.

2.3.1 The Wheatstone Bridge Balance Mode

The central role played by the Wheatstone bridge in measuring strains makes a more detailed mathematical investigation into its operation worthwhile.

Recall that by suitably selecting and adjusting R_1, R_2, R_3 and R_4, it is possible to obtain the equilibrium condition (i.e. I_G=0).

Consider Ohm's law, $V = I \times R$, applied to the sensitive instrument's branch. It is evident that once the bridge is balanced and I_G=0, then V_G, the voltage across the sensitive instrument must, by necessity, be zero i.e. V_G=$I_G R_G$=0.

This condition is equivalent to saying that the voltage at point A (i.e. V_A) equals the voltage at point C (i.e. V_C). If the voltages at these two points are equal, then it follows that the voltage drop from B to A ($V_{B\text{-}A}$=$I_1 R_1$) must be equal to the voltage drop from B to C ($V_{B\text{-}C}$=$I_2 R_2$). Similar relations apply to the voltage drops from point D to A and D to C.

Furthermore, since no current passes through the sensitive instrument's branch at the balance conditions, the current flowing through R_1 must be equal to the current flowing through R_4 and the current flowing through R_2 must be equal to the current flowing through R_3 [3]. From the above observations, we could write:

$$E_{B-A} = E_{B-C}$$

$$\Rightarrow I_1 R_1 = I_2 R_2 \tag{2.4}$$

$$E_{D-A} = E_{D-C}$$

$$\Rightarrow I_1 R_4 = I_2 R_3 \tag{2.5}$$

$$\frac{(2.4)}{(2.5)} \Rightarrow \frac{I_1 R_1}{I_1 R_4} = \frac{I_2 R_2}{I_2 R_3}$$

$$\frac{R_1}{R_4} = \frac{R_2}{R_3} \tag{2.6}$$

$$R_1 = \left(\frac{R_2}{R_3}\right) R_4 \tag{2.7}$$

It is this condition of balance established above that was implicitly used to write equation 2.3.

Recall that R_1 is the resistance of the strain gauge (assuming a quarter bridge configuration). The goal in establishing this relationship is not to compute R_1 or any of the other resistances, but to instrument changes in the value of R_1 (i.e. ΔR_1) for strain purposes.

For the moment, consider that R_2 and R_3 are fixed in values and R_4 is a variable resistor. As observed earlier, the balance condition would be achieved by adjusting R_4 until I_G=0.

Now consider that the strain gauge R_1 is bonded to a test specimen. If the specimen were strained and or subjected to a varying temperature field, a resultant change in the resistance of R_1 would occur according to the relation

$$\Delta R_1 = R_1 G \times \frac{\Delta L}{L} \tag{2.8}$$

This change, although it is a few hundredths of ohm (typically), would upset equation 2.7 and unbalance the bridge.

This loss of equilibrium is indicated by the departure of the reading on the sensitive instrument from the zero mark. By readjusting (varying) R_4, the bridge can be brought back to equilibrium and equation 2.7 would be re-established [3].

The accurate calibration of the resistor R_4 would help determine its precise resistance value irrespective of the point of adjustment. The values of R_4 before and after straining can be successively substituted into equation 2.7 and the respective values of R_1 computed. The difference between the values of R_1 before and after straining will be the value of ΔR_1 in equation 2.8. This quantity can then be substituted into equation 2.2 to compute the strain.

Alternatively, instead of calibrating R_4 in terms of resistance, it can be calibrated directly in micrometers per meter of strain. This holds because the amount of adjustment required in R_4 is obviously related to the resistance change in R_1, and hence to the strain itself [3]. In this case, the micrometer reading of R_4 would be noted when the bridge is initially balanced and the strain gauge R_1 unstrained, then after straining, R_4 is readjusted to balance the bridge and the second micrometer reading noted. The difference between these two readings is equal to the net strain undergone by the strain gauge. It is a helpful practice to place a high resistance variable shunt resistor across R_4, since the actual changes in resistance encountered are very small [3].

There is another method to instrument strains which is different from the two already enumerated above. In this method, instead of rebalancing the Wheatstone bridge after loading the test piece on which the strain gauge has been bonded, the sensitive instrument's reading itself might be taken as a measure of the strain [3]. For small changes in the resistance of the gauge, R_1 (corresponding to moderate strains), the sensitive instrument's reading is proportional to the resistance change or strain. This method would be more convenient if the sensitive instrument were calibrated in units of

micrometers per meter of strain since it is strain corresponding to the resistance change that is being sought [3].

2.3.2 Theory of an Unbalanced Wheatstone Bridge

Consider the diagram of figure 2, and consider the bridge to be unbalanced. It should be noted that equation 2.7 is not applicable to the unbalanced bridge.

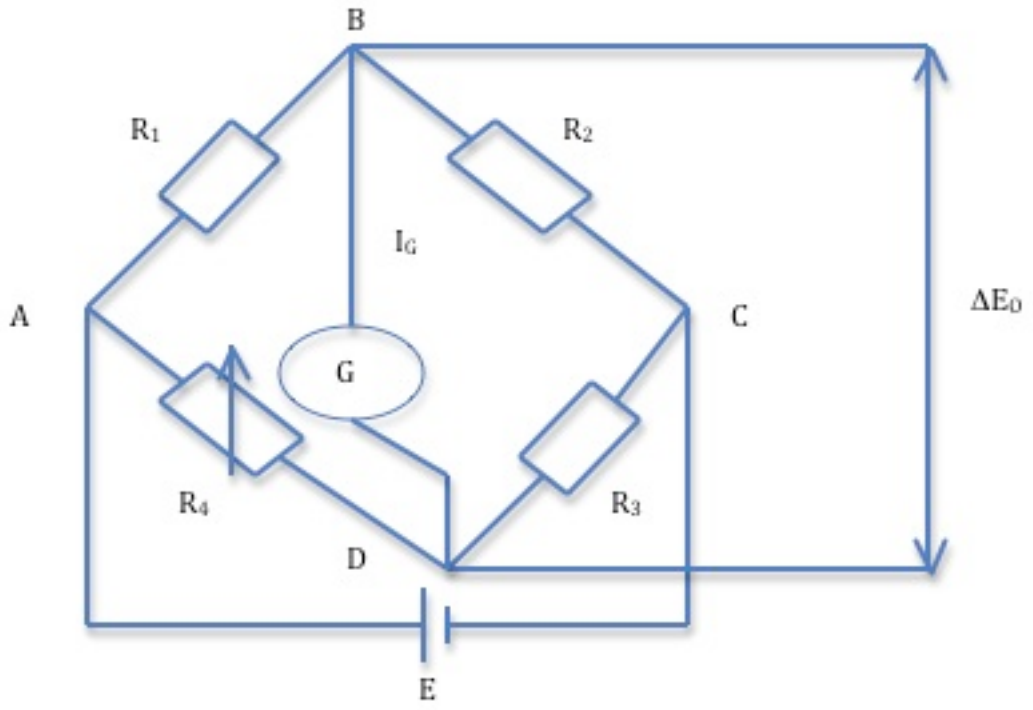

Fig. 2. An unbalanced Wheatstone bridge circuit

The above electrical network can be analyzed using Kirchhoff's current law (KCL) and Kirchhoff's voltage law (KVL) to derive equations that pertain to the unbalanced bridge. Applying KVL and KCL to all electrically complete loops (paths), we obtain:

$$I_1 R_1 + \left(I_1 - I_G\right) R_4 = E$$

$$I_1 R_1 + I_1 R_4 - I_G R_G = E$$

$$I_1 \left(R_1 + R_4\right) - I_G R_G = E \tag{2.9}$$

$$I_1 R_1 + I_G R_G - I_2 R_2 = 0 \tag{2.10}$$

$$\left(I_1 - I_G\right) R_4 - \left(I_G + I_2\right) R_3 - I_G R_G = 0$$

$$I_1 R_4 - I_G R_4 - I_G R_3 - I_2 R_3 - I_G R_G = 0$$

$$I_1 R_4 - I_2 R_3 - I_G \left(R_4 + R_3 + R_G\right) = 0$$

$$-I_1 R_4 + I_2 R_3 + I_G \left(R_4 + R_3 + R_G\right) = 0 \tag{2.11}$$

Using the method of determinants, equations 2.9–2.11 can be solved for I_G. The solution for I_G is given below.

$$I_G = \frac{E\left(R_2 R_4 - R_1 R_3\right)}{R_2\left(R_G + R_3 + R_4\right)\left(R_1 + R_4\right) + R_1 R_3 R_4 - R_2 R_4^2 + R_G R_3\left(R_1 + R_4\right)} \tag{2.12}$$

If the bridge were balanced, then $R_1R_3=R_2R_4$ holds, and hence the numerator would be zero, thus $I_G=0$ [3].

Using equation 2.12, variations in I_G can be observed by straining and changing the resistance of the strain gauge, R_1.

As a numerical example, consider an application in which the following variables apply:

$R_1 = R_2 = R_3 = R_4 = 350\Omega$

$R_G = 150\Omega$

R_G: Sensitive instrument's resistance.

Substituting these values into equation 2.12 yields

$$I_G = \frac{1102500 - 3150R_1}{104125000 + 297500R_1 + 122500R_1 - 42875000 + 52500R_1 + 18375000}$$

$$I_G = \frac{1102500 - 3150R_1}{79625000 + 472500R_1}$$

$$I_G = \frac{4410 - 12.6R_1}{318500 + 1890R_1} \tag{2.13}$$

For example, given that R_1 (350Ω) is an active gauge and the other resistors are fixed (350Ω), with sensitive instrument resistance of 150Ω, then the current output of the bridge which is proportional to the strain on R_1 is given by equation 2.13.

Given the expressions for the current or voltage output of a Wheatstone bridge, then the bridge sensitivity is equivalent to the slope of the I_G versus R_1 curve or the slope of ΔE_o versus R_1.

2.4 Strain Gauge Operation Theory

The total electrical resistance of a conductor of uniform cross-section is given by the expression below [2].

$$R = \frac{\rho L}{A} \tag{2.14}$$

Where:

R: Resistance (Ω)

ρ: Specific resistance (Ωm)

A: Area (m^2).

Taking logarithms and differentiating equation 2.14 leads to

$$\ln R = \ln \rho + \ln L - \ln A$$

$$\frac{1}{R} dR = \frac{1}{\rho} d\rho + \frac{1}{L} dL - \frac{1}{A} dA \tag{2.15}$$

For the case of a uniaxial tensile stress state, we have the following as in [2].

$$\varepsilon_a = \frac{dL}{L}$$

$$\varepsilon_t = -\upsilon \varepsilon_a = -\upsilon \frac{dL}{L}$$

Where:

ε_a: Axial strain in the conductor

ε_t: Transverse strain in conductor

υ: Poisson's ratio

If the diameter of the conductor before and after the application of the axial strain is d_o and d_f respectively, then d_f is given by the expression below [1].

$$d_f = d_o \left(1 - \upsilon \frac{dL}{L}\right) \tag{2.16}$$

Also, the cross-sectional area of the conductor before (A_o) and after (A_f) are given by:

$$A_o = \frac{\pi d_o^2}{4}$$

$$A_f = \frac{\pi d_f^2}{4}$$

Hence,

$$\frac{dA}{A} = \frac{\pi d_f^2 / 4 - \pi d_o^2 / 4}{\pi d_o^2 / 4}$$

$$\frac{dA}{A} = \frac{d_f^2 - d_o^2}{d_o^2}$$

$$\frac{dA}{A} = \left(\frac{d_f}{d_o}\right)^2 - 1$$

$$\frac{dA}{A} = \left(1 - \upsilon\frac{dL}{L}\right)^2 - 1$$

$$\frac{dA}{A} = \left[1 - 2\upsilon\frac{dL}{L} + \upsilon^2\left(\frac{dL}{L}\right)^2\right] - 1$$

$$\frac{dA}{A} \approx -2\upsilon\frac{dL}{L} \tag{2.17}$$

Substituting equation 2.17 into 2.15 gives:

$$\frac{dR}{R} = \frac{d\rho}{\rho} + \frac{dL}{L}(1 + 2\upsilon) \tag{2.18}$$

Assuming that the change in length and the change in the specific resistance are small, then higher order terms in equation 2.18 can be neglected leading to

$$\frac{\Delta R}{R} = \frac{\Delta\rho}{\rho} + (1 + 2\upsilon)\frac{\Delta L}{L}$$

$$\frac{\Delta R}{R} = \frac{\Delta\rho}{\rho} + (1 + 2\upsilon)\varepsilon_a \tag{2.19}$$

To describe the change in the electrical resistance of a conductor caused by its change in length, strain sensitivity is introduced.

Dividing both sides of equation 2.19 by the axial strain ε_a gives

$$\frac{dR/R}{\varepsilon_a} = \frac{\Delta R/R}{\varepsilon_a} = \frac{d\rho/\rho}{\varepsilon_a} + (1+2\upsilon)$$

$$G = \frac{\Delta\rho/\rho}{\varepsilon_a} + (1+2\upsilon) \qquad (2.20)$$

G is the sensitivity of the metal or alloy used for the conductor of the gauge as stated in equation 2.1.

From equation 2.20, we find that the strain sensitivity of a strain gauge is produced by two factors [1]:

1. The term $\frac{\Delta\rho/\rho}{\varepsilon}$ representing the change in the specific resistance of the conductor material
2. The term (1+2υ) representing the change in the conductor's dimensions

The change in the specific resistance is due to variations in the number of free electrons and their increased mobility with applied strain [1].

A strain gauge exhibits a rate of resistance change $\Delta R/R$ that is related to the strain ε in the direction of the grid lines, as expressed by equation 2.2.

The gauge factor or calibration constant (G) of the gauge varies for different gauge materials/compositions as shown in Table 1.

2.5 Voltage Output of an Unbalanced Wheatstone Bridge

Consider the basic Wheatstone bridge circuit, with one active resistance, R_1 (strain gauge).

The output voltage is derived as follows:

$$\Delta E_O = \frac{\left(R_1 + \Delta R_1\right)\left(R_3 + \Delta R_3\right) - \left(R_2 + \Delta R_2\right)\left(R_4 + \Delta R_4\right)}{\left(R_1 + \Delta R_1 + R_2 + \Delta R_2\right)\left(R_3 + \Delta R_3 + R_4 + \Delta R_4\right)} E$$

$$\Delta E_O = \frac{R_1R_3 + R_1\Delta R_3 + R_3\Delta R_1 + \Delta R_1\Delta R_3 - R_2R_4 - R_2\Delta R_4 - R_4\Delta R_2 - \Delta R_2\Delta R_4}{R_1R_3 + R_1\Delta R_3 + R_1R_4 + R_1\Delta R_4 + R_3\Delta R_1 + \Delta R_1\Delta R_3 + R_4\Delta R_1 + \Delta R_1\Delta R_4 + R_2R_3 + R_2\Delta R_3 + R_2R_4 + R_2\Delta R_4 + R_3\Delta R_2 + \Delta R_2\Delta R_3 + R_4\Delta R_2 + \Delta R_2\Delta R_4} E \qquad (2.21)$$

Using $R_1R_3 = R_2R_4$ and neglecting smaller terms (first and second order) in the denominator, the expression simplifies to

$$\Delta E_O = \frac{R_1R_2\left[\frac{\Delta R_1}{R_1} - \frac{\Delta R_2}{R_2} + \frac{\Delta R_3}{R_3} - \frac{\Delta R_4}{R_4}\right] \times \frac{R_4}{R_1} E}{R_1R_3 + R_1R_4 + R_2R_3 + R_2R_4}$$

$$\Delta E_O = \frac{R_1R_2\left[\frac{\Delta R_1}{R_1} - \frac{\Delta R_2}{R_2} + \frac{\Delta R_3}{R_3} - \frac{\Delta R_4}{R_4}\right] \times \frac{R_4}{R_1} E}{R_3\left(R_1 + R_2\right) + R_4\left(R_1 + R_2\right)}$$

$$\Delta E_O = \frac{R_1R_2\left[\frac{\Delta R_1}{R_1} - \frac{\Delta R_2}{R_2} + \frac{\Delta R_3}{R_3} - \frac{\Delta R_4}{R_4}\right] \times \frac{R_4}{R_1} E}{\left(R_1 + R_2\right)\left(R_3 + R_4\right)}$$

$$\Delta E_O = \frac{\frac{R_1R_2}{\left(R_1 + R_2\right)}\left[\frac{\Delta R_1}{R_1} - \frac{\Delta R_2}{R_2} + \frac{\Delta R_3}{R_3} - \frac{\Delta R_4}{R_4}\right]\frac{R_4}{R_1} E}{\left(R_3 + R_4\right)} \qquad (2.22)$$

But we also have

$$R_1R_3 = R_2R_4$$

$$R_1R_3 + R_1R_4 = R_2R_4 + R_1R_4$$

$$R_1\left(R_3 + R_4\right) = R_4\left(R_1 + R_2\right)$$

$$R_3 + R_4 = \frac{R_4}{R_1}\left(R_1 + R_2\right)$$

Hence,

$$\Delta E_O = \frac{\dfrac{R_1R_2}{\left(R_1 + R_2\right)}\left[\dfrac{\Delta R_1}{R_1} - \dfrac{\Delta R_2}{R_2} + \dfrac{\Delta R_3}{R_3} - \dfrac{\Delta R_4}{R_4}\right]\dfrac{R_4}{R_1}E}{\dfrac{R_4}{R_1}\left(R_1 + R_2\right)}$$

$$\Delta E_O = \frac{R_1R_2}{\left(R_1 + R_2\right)^2}\left[\frac{\Delta R_1}{R_1} - \frac{\Delta R_2}{R_2} + \frac{\Delta R_3}{R_3} - \frac{\Delta R_4}{R_4}\right]E \tag{2.23}$$

Letting $r = R_2 / R_1$, then we can write ΔE_o as

$$\Delta E_O = \frac{R_2/R_1}{1/R_1\left(R_1 + R_2\right)^2}\left[\frac{\Delta R_1}{R_1} - \frac{\Delta R_2}{R_2} + \frac{\Delta R_3}{R_3} - \frac{\Delta R_4}{R_4}\right]E$$

$$\Delta E_O = \frac{r}{\left(\dfrac{R_1 + R_2}{R_1}\right)^2}\left[\frac{\Delta R_1}{R_1} - \frac{\Delta R_2}{R_2} + \frac{\Delta R_3}{R_3} - \frac{\Delta R_4}{R_4}\right]E$$

$$\Delta E_O = \frac{r}{\left(1 + r\right)^2}\left[\frac{\Delta R_1}{R_1} - \frac{\Delta R_2}{R_2} + \frac{\Delta R_3}{R_3} - \frac{\Delta R_4}{R_4}\right]E \tag{2.24}$$

The output voltage of a bridge is a linear function of changes in resistances (i.e. with the higher order terms ignored) [1,2]. This output is typically in the neighborhoods of

millivolts and microvolts due to the small nature of the change in resistance producing the output. The ratio of the bridge output voltage (ΔE_o) to the excitation/supply voltage (E) is an indication of the strain causing the change in the bridge's output.

2.6 Performance of the Wheatstone Bridge

There are some concerns in the operation of the Wheatstone bridge. For instance, we would be interested to know how the excitation voltage affects the bridge's output.

Also, how would the sensitive instrument's and strain gauge resistance affect the output?

These concerns are critical for unbalanced bridge conditions only since there is no output when the bridge is balanced.

Therefore, under equilibrium conditions, the bridge is absolutely unaffected by either excitation voltage or the sensitive instrument's resistance. Because bridge performance is completely independent of the excitation voltage when the bridge is balanced, the method of rebalancing the bridge for each strain reading is mostly where the highest accuracy is required [3].

Whenever the bridge is unbalanced, the factor $R_1R_3–R_2R_4$ is not equal to zero and the bridge output in terms of sensitive instrument's current is directly proportional to the excitation voltage. This is a possible source of error when the instrument is calibrated to read strain directly without rebalancing [3].

With a sensitive instrument's impedance of zero, there would be no voltage difference between points A and C of the bridge. From this, it is clear that the voltage difference

between these two points would be greatest (i.e. maximum possible output) for a given strain if the impedance of the sensitive instrument were infinite [3].

Consider a sensitive instrument of infinite impedance. The voltage difference between points A and C is computed as

$$E_{A-C} = I_1 R_1 - I_2 R_2$$

But if no current passes through the sensitive instrument (i.e. I_G=0), we would have:

$$I_1 = \frac{E}{R_1 + R_4}$$

$$I_2 = \frac{E}{R_2 + R_3}$$

Therefore we obtain E_{A-C} as

$$E_{A-C} = \frac{ER_1}{R_1 + R_4} - \frac{ER_2}{R_2 + R_3} \tag{2.25}$$

Differentiating equation 2.25 with respect to R_1, we obtain:

$$\frac{dE_{A-C}}{dR_1} = \frac{\left(R_1 + R_4\right)E - ER_1}{\left(R_1 + R_4\right)^2}$$

$$dE_{A-C} = \frac{ER_4}{\left(R_1 + R_4\right)^2} dR_1 \tag{2.26}$$

From equation 2.1 we get the following expression for *dR:*

$$dR = \frac{dL}{L} GR$$

Substituting the above relation into equation 2.26 gives

$$dE_{A-C} = \frac{R_1 R_4}{\left(R_1 + R_4\right)^2} GE \frac{dL}{L} \tag{2.27}$$

Equation 2.27 is the equation of the change in voltage drop across a sensitive instrument of infinite impedance [3].

For small changes in resistance, the output voltage is proportional to the excitation voltage, gauge factor and strain.

If R_1 and R_4 have the same nominal value, then equation 2.27 simplifies to

$$dE_{A-C} = \frac{ER_1^2}{\left(2R_1\right)^2} G \frac{dL}{L}$$

$$dE_{A-C} = \frac{E}{4} G \frac{dL}{L} \tag{2.28}$$

In equation 2.28, the bridge output is independent of the resistances of the arms of the bridge, so long as these resistances are nominally equal to each other.

Chapter 3

Strain Gauge Measurement Errors and Correction Methods

3.1 Critical Issues Involving the Use of Strain Gauges in SHM-based Applications

There are potentially numerous sources of error in strain gauge measurement applications [3,4,5,6,7]:

- Apparent strain (thermal output);
- Heating effects on gauge due to excitation voltage;
- Transverse sensitivity effects;
- Gauge factor variation;
- Lead wire effects;
- Moisture and humidity effects;
- Other factors e.g. precision of the Poisson ratio.

These sources of error must be taken into account in an attempt to obtain more accurate measurements.

3.1.1 Apparent Strain/ Thermal Output

Strain gauges used in various applications can hardly experience a constant temperature field in the course of data acquisition [10]. The fluctuation of the surrounding temperature of the gauge induces strain in the strain gauge (due to changes in resistance), which are not stress-related. Thermal output would arise although a strain gauge may have been connected to a strain indicator and balanced, as long as there changes in the

reference temperature of the gauge [7]. This temperature-induced strain is independent of, and unrelated to, the mechanically induced strain in the test piece to which the gauge is bonded [7,13]. Thus, it is an erroneous component of the overall strain reading used for stress evaluations [13].

This purely temperature-induced strain is termed thermal output or temperature-induced apparent strain.

As the temperature of the gauge's environment increases, the temperature gradient between the grid material of the gauge and the test specimen also increases. This temperature difference becomes more pronounced with increasing surrounding temperatures because the backing materials, which electrically insulate the gauges from the test specimen, are good thermal insulators as well.

Conventional strain correction procedures currently do not take into consideration this temperature gradient because it is assumed that the strain gauge grid material and the test specimen are at the same temperature. As a result of this, substantial errors of a few hundred micro strains may be acquired in the strain measurements.

Thermal outputs in strain gauges is the result of contributions due to changes in the grid resistance of the strain gauge as a result of temperature changes and the differential thermal expansion between the grid conductor of the gauge and the material of the test sample.

With changes in temperature, the test specimen expands or contracts. Since the gauge is firmly bonded to the test specimen, it expands or contracts with the test specimen [7].
The contributors to the thermal output may be positive or negative in sign with reference to the sign of the temperature change, thus the net thermal output is the algebraic sum of the contributors [7].

There are many factors influencing the thermal output of strain gauges; material of the test specimen, grid alloy and lot of gauge, gauge series and pattern, transverse sensitivity of gauge, bonding and encapsulating materials, and installation procedures [7].
It is very difficult to predict the exact thermal output of any gauge bonded to a test structure since there are always differences in the thermal expansion characteristics of materials from lot to lot. A very useful practice therefore is to evaluate the thermal output behavior of one or more gauges under thermal conditions or environments likely to be encountered in practice [7].

These errors should be controlled and or compensated for to obtain the true strain state of the test specimen caused by mechanical loads.
Errors due to thermal output can become extremely large as temperatures deviate from the reference temperature, and as such, can compromise the precision of measurements [7].
To minimize the thermal output, the thermal expansion coefficients of the grid material of the gauge and the material of the test sample should be matched as discussed in section 3.2.

Among all the potential sources of error, apparent strain is said to be the most serious and most commonly encountered of all in strain measurement readings [6,7,13]. This error as pointed out earlier arises as a result of changing temperature conditions of the gauge's environment. Changes in temperature affect the gauge reading in two ways. The first is change in the sensitivity of the gauge. Often, the gauge factor decreases with increasing temperature. The second is the thermal output due to the changes in temperature.

This work seeks to address errors arising from apparent strains and the heating effects resulting from the excitation voltages. Due experimental practices are observed so that errors from other sources are minimized or eliminated.

There is limited information in the literature dealing with the correction of errors caused by transient heating in electrical resistance strain gauge measurement applications [4].

The objectives of this investigation are, therefore, to quantify bonded-wire resistance strain gauge thermal output measurements acquired in a controlled temperature environment, and to propose correction models applicable to current test programs.

3.1.2 Heating Effects on Gauge Due to Excitation Voltage

Excitation voltages provide energy to the gauges but they also have the effect of causing local heating in the vicinity of strain gauges. In static applications, the tolerable power density, w, of a strain gauge can vary from 20kW/m^2 when bonded to conducting copper to 0.01kW/m^2 in an unfilled polymer [5]. When the gauge forms an active arm of a Wheatstone bridge, the w-values are converted to an allowable bridge supply voltage E, for a given gauge area, A and resistance R, using: $w = E^2 / 4RA$ [5]. Exceeding optimal

values of E would cause considerable self-heating effects [5].

For a disc element under a gauge, the element can be modeled as a two-dimensional heat distribution problem involving a radius, r and a thickness, z [5].

The heat transfer equation is expressed below as in [5].

$$\frac{\delta^2 T}{\delta r^2} + \frac{1}{r}\frac{\delta T}{\delta r} + \frac{\delta^2 T}{\delta z^2} + \frac{H}{k} = \frac{1}{\alpha}\frac{\delta T}{\delta t} \tag{3.1}$$

Where:

H: The heat generated per unit volume in the element to which the strain gauge is bonded

k: The thermal conductivity of the test material to which the gauge is bonded

T: Temperature

t: Time.

For a node directly under the gauge, the heat generated per unit volume in an element is expressed below as in [5].

$$H = \frac{2V_g^2}{RAz} \tag{3.2}$$

Where:

V_g: The voltage across the terminals of the strain gauge (bridge output voltage).

R: The resistance of the gauge

z: The node separation in the thickness direction.

Given that R, A and z are constants for a particular gauge, then the heat generated per unit volume is directly proportional to the square of the excitation voltage [5].

Excessive gauge excitation levels impact the gauge performance adversely [6]. Some of these adverse effects include loss of self-temperature compensation, an increase in hysteresis and creep effects, and a decrease in zero (no load) gauge stability [6].

The first effect is of serious concern in strain gauges used with composite materials since self-temperature-compensation is not normally employed [6]. Hysteresis and creep effects are largely determined by the thermal conductivity behavior of the substrate [6].

3.1.3 Transverse Sensitivity Effects

Ideally, we would desire a strain gauge to respond to strain in the direction of its major axis of strain only. Unfortunately, this is seldom the case. The strain gauge is sensitive to strains in directions other than the principal strain axis. For example, the strain gauge is sensitive to strain in the axis perpendicular to the major strain axis. This phenomenon is referred to as transverse sensitivity [6,13]. Strain acquired as a result of transverse sensitivity effects may or may not be of great concern depending on its magnitude and the desired accuracy in strain measurements.

3.1.4 Gauge Factor Variation With Temperature

The gauge factor of a strain gauge is temperature-dependent. Thus changes in temperature lead to changes in the gauge factor. This subsequently introduces an error component in the acquired strain. Multiplying the measurement values by the ratio of the gauge factor during measurement to the gauge factor setting of the instrument effects gauge factor correction [2,7]. Gauge factor correction may be used where desired [2,7].

3.1.5 Lead Wire Effects

The resistance of lead wires can introduce substantial resistance into the circuit of the gauge thereby altering the nominal resistance of the gauge [8]. This is of particular concern in remote applications where lead wires may need to be of considerable length.

The resistance of a copper wire of length l (meters) and cross section F (mm^2) amounts to [8]:

$$R_l = \frac{l}{57F} \tag{3.3}$$

Just imagine the amount of resistance in the circuit for long copper lead wires! The effects of lead wire resistance on the resistance of the active gauge is also known as lead wire desensitization effects. Correction for lead wire effects may be necessary depending on their potential impact [2,13].

3.1.6 Moisture and Humidity Effects

Sensitivity of strain gauges to moisture and humidity is of concern, especially when long-term measurement is planned, and when environmental conditions may be unfavorable [13].

Moisture can be detrimental to a strain gauge. This comes about as a result of changes in the local properties of the test specimen and the gauge itself due to ingress of moisture and hence changes in the resistance or nominal resistance of the gauge [2,3].

3.1.7 Other Factors

The sources of error in strain gauge measurements discussed here are not exhaustive nor is it meant to be a catalogue of all such sources as there are still other possible sources.

Other factors still influence the precision of strain measurements, for example, the precision with which the Poisson ratio is known. The accuracy of the strain readings in measurement applications is somewhat dependent upon the accuracy with which the Poisson ratio is known. Also, the phenomenon of slip or "gauge creep" can lead to erroneous results. Gauge misalignment can potentially cause erroneous readings [6].

3.2 Methods of Minimizing Errors in Strain Gauge Measurements

There are some opportunities to eliminate or minimize some of the errors in measurement applications.

Some of these methods of ensuring cleaner measurements from strain gauge readings include the following [1,4,7,9,11,12]:

- Self-temperature compensation (STC);
- Dummy gauge method;
- Three lead wire system;
- Wheatstone bridge temperature and nonlinearity compensation;
- Neural network compensation models;
- Optimizing excitation levels.

3.2 .1 Self-Temperature Compensation

Certain metallic alloys are known to minimize the thermal outputs over a wide range of temperature when bonded to test materials with thermal expansion coefficients for which

they are intended [5,6,7]. Strain gauges employing such specially made alloys are known as self-temperature compensated (STC) gauges.

The thermal expansion characteristics of STC gauges are matched to those of the test specimen to which they are bonded so that apparent strains due to the gauge and the specimen are equal but opposite in sign, and hence cancel out approximately. To ensure this, the strain gauge alloy is usually processed so as to minimize the apparent strain due to temperature effects. Self-temperature compensated strain gauges usually come with apparent strain curves, which represent the nominal gauge response with temperature when mounted to the appropriate material.

The contributions to thermal output are caused primarily by the following two factors [7]:

1. Resistivity of the grid conductor is temperature-dependent;
2. There exists a differential thermal expansion between the grid conductor and the material of the test piece.

Mathematically, the unit change in resistance per unit resistance due to temperature effects on the strain gauge is expressed below [7].

$$\left(\frac{\Delta R}{R_o}\right)_{T/o} = \left[\beta_G + G\left(\frac{1+K_t}{1-\upsilon K_t}\right)\left(\alpha_S - \alpha_G\right)\right]\Delta T \tag{3.4}$$

$\left(\frac{\Delta R}{R_o}\right)_{T/O}$: unit change in resistance from reference resistance, R_O

β_G : temperature coefficient of resistance of grid conductor of gauge

K_t : transverse sensitivity of gauge

ΔT: temperature change

(α_S–α_G): difference in thermal expansion coefficients of substrate and grid, respectively

υ: Poison's ratio

G: gauge factor.

Ensuring that α_S and α_G are matched (i.e. they are equal) leads to a zero value for their associated term in equation 3.4.

Depending upon the test temperature, and the degree of precision required in strain measurements, it is some times necessary to compensate for the thermal output, even though STC gauges are used [7].

3.2.2 Dummy Gauge Method

In principle, temperature compensation can be readily accomplished by installing a second strain gauge, called a "dummy gauge" on an unstrained test piece separate from that to which the active strain gauge has been bonded [7,13]. If the two pieces experience the same temperature gradients (changes), then both gauges will register equal but opposite thermal outputs.

Strictly, the dummy gauge must be bonded on a material identical to the test part but connected to the adjacent side of the Wheatstone bridge (e.g. as resistance R_2 in Fig. 1). It must be ensured that the dummy gauge and the active gauge are in the same temperature field. Two other conditions that must be satisfied to obtain accurate thermal compensation include [7,13]:

1. The active and dummy gauges must be identical;

2. The dummy gauge must be made from a material identical to that of the test piece in all characteristics.

Given that these hypothetical conditions are satisfied, the thermal outputs are expected to be identical but opposite in sign [7]. Since identical changes in resistance in the adjacent arms of the bridge occur due to identical temperature conditions, the thermal outputs of the active and dummy gauge are expected to cancel out exactly leaving only the stress-induced strain in the active gauge. To further aid in achieving thermal compensation, it is required that the lead wires to the active and dummy gauges be of the same length and they be routed together [7].

There are a few challenges in this method of temperature compensation. Notable among them is the challenge of establishing and maintaining the ideal conditions postulated above. It is almost impossible to make sure that the unstrained test piece in the test environment is always unstrained [7]. It is also very difficult to ensure that the active gauge and the dummy gauge are always at the same temperature [7,13]. It must also be noted that no two strain gauges are precisely identical even if they are from the same lot [7].

There is a special category of strain measurements that can incorporate a second gauge to achieve thermal compensation [7]. This category consists of those applications in which the ratio of the strains at two different but closely adjacent points (or at least thermally adjacent) on a test piece are known a priori [7]. For example, two gauges (i.e. half-bridge configuration) bonded to opposite sides of a bar experiencing compressive and tensile

forces simultaneously, is automatically temperature-compensated [2,3]. Other examples of measurements in this category include: bars in pure tension, beams in bending, columns and diaphragms [7].

Assume in a Wheatstone bridge circuit that R_2 is installed as a dummy gauge, to work with the active gauge, R_1. Also, assume that R_1 and R_2 are gauges of the same lot number with the same nominal resistance. If R_1 and R_2 experience equal changes in resistance due to temperature changes, then their final resistances will be $R_1+\Delta R_1$ and $R_2+\Delta R_2$ respectively. These changes in resistances are strictly due to temperature changes only. It is observed from the above considerations that $R_1 \approx R_2$ and hence $R_1+\Delta R_1 \approx R_2+\Delta R_2$. This development does not destroy the balance condition

$$\frac{R_1}{R_4} = \frac{R_2}{R_3} \tag{3.5}$$

As long as the equality in equation 3.5 holds, equilibrium persists and there would be no current through the sensitive instrument and the bridge will remain balanced.

If the structure to which the active gauge R_1 has been bonded is simultaneously strained and exposed to temperature variations whilst the dummy gauge is exposed to the same temperature variations only, then the strain indication of the bridge will be unaffected by temperature variations as shown below mathematically [1]. The output of the bridge is as given by equation 2.24:

$$\Delta E_o = \frac{r}{(1+r)^2}\left[\frac{\Delta R_1}{R_1} - \frac{\Delta R_2}{R_2} + \frac{\Delta R_3}{R_3} - \frac{\Delta R_4}{R_4}\right]E$$

$$r = R_2 / R_1$$

Based on the developments above, we would have:

$$\Delta E_O = \frac{1}{4}\left[\left(\frac{\Delta R_1}{R_1}\right)_\varepsilon + \left(\frac{\Delta R_1}{R_1}\right)_{\Delta T} - \left(\frac{\Delta R_2}{R_2}\right)_{\Delta T}\right]E$$

$$\Delta E_O = \frac{1}{4}\left[\left(\frac{\Delta R_1}{R_1}\right)_\varepsilon\right]E \tag{3.6}$$

Temperature compensation is thus achieved with the dummy gauge.

3.2.3 Three Lead Wire System

The resistances (r_1+R_1) and (r_2+R_2) are connected to adjacent arms of the bridge. They have equal but opposite effects, which cancel out. However, r_3 is connected to the output of the bridge, thus it has no effect on the measurements yet it compensates for lead wire effects [1,7]. This is shown in the following circuit diagram.

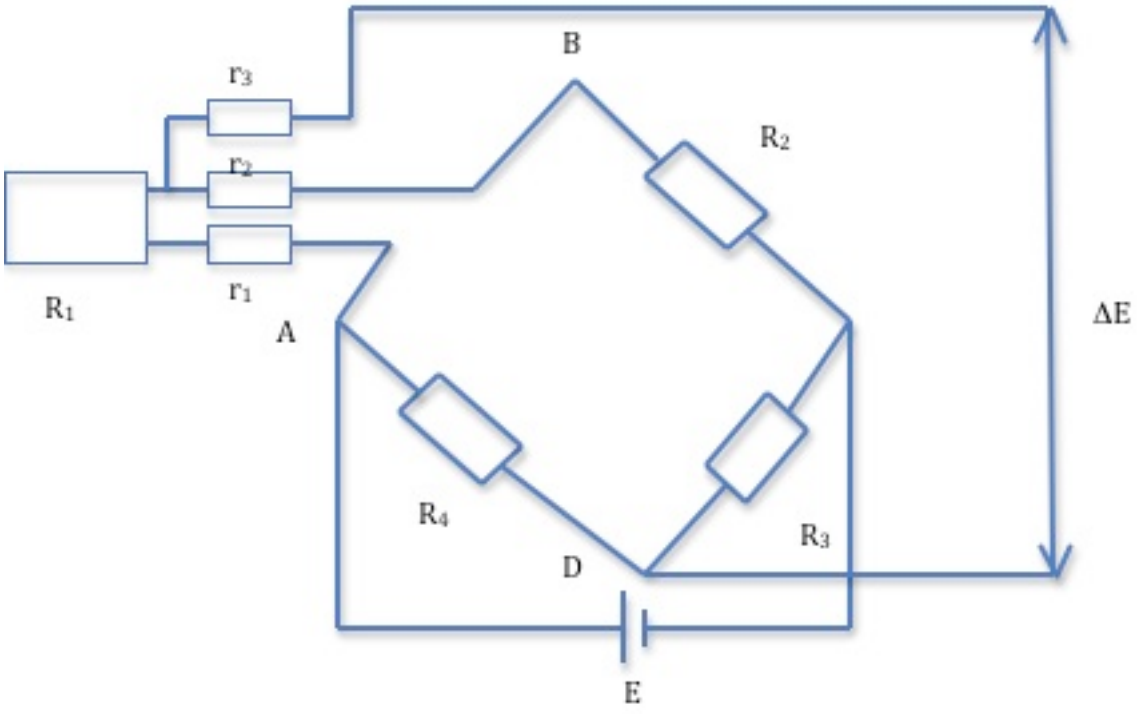

Fig. 3. A three lead wire gauge system

Consider the output of the Wheatstone bridge above with one active strain gauge, R_1. This is given by equation 2.24 as stated below.

$$\Delta E_o = \frac{r}{(1+r)^2}\left[\frac{\Delta R_1}{R_1} - \frac{\Delta R_2}{R_2} + \frac{\Delta R_3}{R_3} - \frac{\Delta R_4}{R_4}\right]E$$

$$r = R_2 \big/ R_1$$

For the three lead wire system, the equation becomes

$$\Delta E_O = \frac{R}{(1+r)^2}\left[\frac{\Delta R_g}{R_g} + \left(\frac{\Delta R_g}{R_g}\right)_T + \left(\frac{\Delta R_L}{R_L}\right)_T - \left(\frac{\Delta R_2}{R_2}\right)_T - \left(\frac{\Delta R_L}{R_L}\right)_T\right]E \tag{3.7}$$

$R_1=R_g$ (resistance of gauge).

$R_L=r_1=r_2$.

Since $R_1=R_2$, equation 3.7 simplifies to

$$\Delta E_o = \frac{1}{4}\left[\frac{\Delta R_g}{R_g}\right]E \tag{3.8}$$

Hence temperature compensation is achieved!

3.2.4 Wheatstone Bridge Temperature and Nonlinearity Compensation

Thermal stability of the strain gauge and Wheatstone bridge is of great concern in strain measurement applications. This is so because gauges and bridges often have to operate in environments that experience temperature fluctuations regularly and as a result adequate temperature compensation of the Wheatstone bridge and the gauge(s) is an absolute necessity for accurate measurement of strains. The need for temperature compensation of strain gauges is necessitated by the following factors:

1. The fact that the resistance of most gauges change with temperature;
2. The fact that the thermal expansion coefficients of the strain gauge material and that of the test piece may not be matched.

The sensitivity S_s of a strain gauge Wheatstone-bridge system is defined as the product of the sensitivity of the gauge, G and the sensitivity of the bridge circuit, S_c [1].

Thus

$$S_s = GS_c = \frac{\Delta R_g / R_g}{\varepsilon} \frac{\Delta E_o}{\Delta R_g / R_g} \tag{3.9}$$

Where $\frac{\Delta E_O}{\Delta R_g / R_g}$ is the sensitivity of the bridge circuit.

Evaluating S_s for a quarter bridge configuration (i.e. R_1 is the gauge's resistance) gives the expression below [1].

$$S_s = \frac{r}{1+r} G \sqrt{P_g R_g} \tag{3.10}$$

P_g : power that can be dissipated by gauge

Now, for a half-bridge configuration (active gauge in arm R_1 and dummy gauge in arm R_2), and with r =1, the sensitivity is

$$S_s = \frac{1}{2} G \sqrt{P_g R_g} \tag{3.11}$$

From equation 3.11, it is realized that placing the dummy gauge in arm R_2 of the Wheatstone bridge to achieve temperature compensation reduces the circuit efficiency to 50% [1]. To avert this undesirable situation, the dummy gauge is placed in arm R_4 instead

of arm R_2 of the Wheatstone bridge [1]. If all four arms of the bridge are active gauges, then improved system sensitivity is achieved in addition to temperature compensation.

From equation 3.10, it is clear that increasing P_g *(E)* would increase the sensitivity of the system. However, there is a limit to the amounts of power that can be handled safely and with minimum errors since increasing P_g also increases the thermal output.

For the case where two or four gauges are used in the bridge with the test part, the gauges do not even need to be STC by construction and such a bridge is still temperature-compensated.

Wheatstone bridge nonlinearity effects must be considered and compensated for when large strains (e.g. 5% or greater) are to be measured with an unbalanced Wheatstone bridge [2]. Bridge nonlinearity compensation expressions exist for all bridge configurations (i.e. quarter, half and full) [2,14].

3.2.5 Neural Network Compensation Models

Given parameters *X* and *Y* to be approximately linear functions of both strain variations δε (with reference to 0 με) and temperature variations δT (with reference to 0 °C), and are measureable, then a neural network can be trained with the data set {(X, Y), (δε,δT)}, obtained from experiments [12]. Suitable network architectures and training algorithms can be used [11,12].

Optimal parameters for network performance can be found by comparing performance at different parameter values and the best network chosen for the compensation scheme

[11,12]. Neural networks may prove to offer comparable or better solutions to the thermal compensation problem, hence that opportunity should be explored.

3.2.6 Optimizing Excitation Levels

The heating effects of excitation voltages are well known [5,6,9]. It is therefore imperative to use excitation levels that allow for good signal levels and at the same time minimize heating effects. This is particularly true with strain gauges mounted to materials of low conductivity because the heating effects become localized in the vicinity of the strain gauge, thereby making the heating effects of the excitation voltage more pronounced.

As a general rule for minimizing the heating effects of excitation levels, gauges of higher resistances are desirable. This permits relatively high bridge excitation levels while still maintaining low current levels, where desired [6]. This also allows for good gauge stability while still allowing reasonable gauge sensitivity [6].

Higher gauge resistances also have the added benefit of decreasing lead wire resistance effects and unwanted signal variations caused by changes in lead wire resistances that come from temperature fluctuations [13].

3.3 Correction Theory

With the opportunities available to minimize errors in strain readings we can choose to employ them before measurements are taken so that we may obtain measurements with minimal errors. This way, we may not do any further cleaning of the measurements

because of the measures put in place before the readings were taken. I refer to this approach as the *control and measure* approach.

There is a second alternative whereby measurements are taken mostly without, or with few correction measures put in place. When such measurements are taken, we estimate the values of potential sources of error present and correct for them. I refer to this approach as *measure and correct* approach.

A third alternative exists. This puts in measures to control errors before measurements are taken and then seeks to correct for remaining errors after measurements are taken. The approach used in this work is the third alternative.

3.3.1 Conventional Correction Theory

The strain indication of a strain gauge in a varying-temperature environment consists of two main components as indicated in the following equation below [4].

$$\varepsilon_{ind}(\Delta T) = \varepsilon_{\sigma}(\Delta T) + \varepsilon_{app}(\Delta T) \tag{3.12}$$

The first term $\varepsilon_{\sigma}(\Delta T)$ in equation 3.12 is stress-induced. It is expressed as a function of the temperature change of the material and reflects the true stress state of the test specimen. Externally applied mechanical loads mainly cause this strain [4,7].

In the experimental scenarios covered in this work, the test part is not loaded mechanically/physically (i.e. it is not stressed) and as a result it is expected that the related term in equation 3.12 should be identically zero.

The second term, apparent strain, is caused by the strain gauge being subjected to a varying temperature gradient as already discussed. This strain can be obtained from equations 3.4 and 3.12 as shown below, upon neglecting transverse sensitivity effects.

$$\varepsilon_{app} = \frac{\left(\Delta R/R_o\right)_{T/o}}{G} = \left[\left(\alpha_S - \alpha_G\right) + \frac{\beta_G}{G}\right]\Delta T \tag{3.13}$$

It should not be assumed in equation 3.13 that the apparent strain is a linear function of temperature, because all of the coefficients are themselves functions of temperature [4,7].

Ideally, a strain gauge sensor bonded to a test specimen would sense only the applied strain of the test specimen and remain unaffected by other variables in the environment [7]. Admittedly, its behavior is far from the ideal. The electrical resistance of the gauge not only changes with strain, but also, with temperature. The gauge factor of the strain gauge itself varies with temperature. These deviations from the ideal can be substantial and can thus cause serious errors if not properly accounted for [7].

It is desirable that the strain gauge should sense only the load or stress-induced strain in equation 3.12. But as already pointed out, that is not the case. The objective of this study

therefore is to obtain the apparent strains expressed by equation 3.13 and model them so as to be able to correct for them.

Chapter 4

Experimental Procedure and Models for Characterizing Apparent Strains Due to the Heating Effects of Excitation Voltages and Temperature Variations

4.1 Experimental Setup

The experimental setup consists of National Instruments Compact Real Time Input Output (cRIO)-9012 controller, strain gauge modules (NI 9237), a thermocouple module (NI 9211), quarter bridge completion blocks (NI 9945), STC gauges (350Ω), thermocouples (J-type), an environmental chamber, a DC power supply and NI LabVIEW 2010 development suite on a computer.

In order to acquire data, the NI 9237 and 9211 modules are placed in slots in the chassis of a National Instruments Compact RIO (NI cRIO-9012) controller. Each NI 9237 module has four channels, which are connected by RJ 50 cables through NI 9945 modules to the strain gauges. Each channel on the NI 9327 modules has built in resistors, forming part of a Wheatstone bridge. External circuitry is then provided alongside the built in resistors for quarter, half or full bridge configurations. Quarter bridge configurations were setup in these experimental situations by providing external strain gauges (350Ω) connected through RJ 50 cables to the NI 9237 modules via the quarter bridge completion blocks (NI 9945). The NI 9237 modules may be powered internally by the NI cRIO-9012 or by supplying an external excitation through connectors on the NI 9237 modules themselves. Thermocouples on the test piece were connected to channels

on the NI 9211 module directly. Each channel on the NI 9211 module has two terminals, one for connecting the positive lead of the thermocouple and the other for the negative lead.

The descriptions of the other components involved in the experimental work are provided in the following sections.

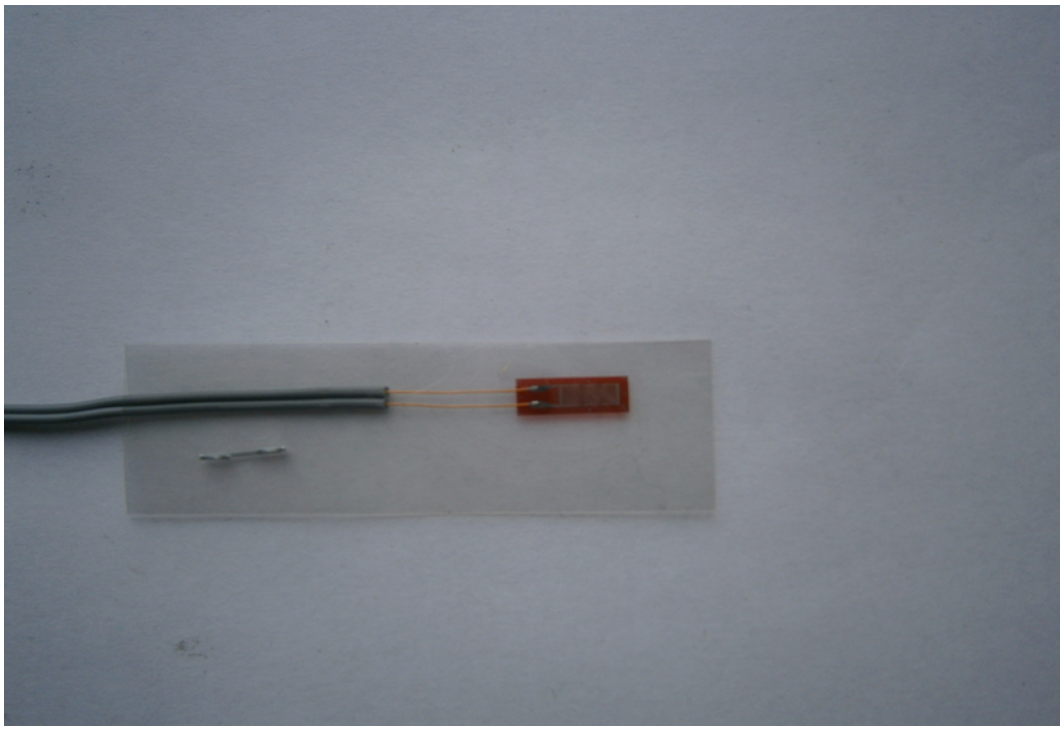

Fig. 4. A Strain gauge

4.1.1 Test Specimen Preparation

Before the sensors were bonded on the test piece, certain surface requirements had to be met in order that good and effective bonds between the sensors and the surfaces may be ensured [1,2,3,8]. Additionally, the surfaces on which the sensors are to be mounted should be even or smooth in a general sense, but not too highly polished, since this inhibits adhesion. These precautions were observed to obtain proper bonding jobs [3].

Fig. 5. Steel test piece at initial stages

All scale, rust, paint and other irregularities were removed from the test surfaces. It was necessary to lightly grind off spots a little larger than the sensors for bonding purposes. Surfaces that were highly polished to start with were roughened slightly, so that good bonds could be achieved [3].

For surfaces that were approximately the right degree of roughness to start with, then it sufficed to do a thorough cleaning job. Sensors will not adhere (bond) well except to clean surfaces. Some volatile solvents such as carbon tetrachloride (CCl_4), acetone, neutralizers and alcohol are adequate for these cleaning purposes.

To secure maximum adhesion between the sensors and the prepared surfaces, it is imperative that cleanliness be maintained until they are firmly in place [3]. Clean solvents

and clean cloths (tissues) were used and fingers kept off the prepared surfaces on the test piece for sensors and the surfaces of the sensors themselves especially the backs of the gauges. In cleaning with the cloth/tissue, one cloth/tissue was used per wipe of a surface. The cloth/tissue was adequately moistened with the solvent, and then the moistened part was applied gently and slowly to the spots to be occupied by the sensors in one direction only. This hopefully, prevented smearing the surfaces on which the sensors were mounted.

The cleaning agents were kept away from the sensors since they would dissolve the cement used in the construction of the sensors, especially the strain gauges, when they come into contact. It is good practice however to wipe the back of the gauges with a cloth slightly dampened with the adhesive to promote good bond formation [3].

With these preparations completed, the sensors were then ready to be cemented in place.

4.2 Bonding Sensors to the Test Specimen

4.2.1 Bonding Strain Gauges

The proper bonding of a strain gauge to a test specimen is perhaps one of the most critical steps in the entire course of measuring strains with bonded resistance strain gauges since there is no way to compensate for errors induced as a result of inadequate or inaccurate execution of the bonding process.

Selection of the proper adhesive for bonding is strongly dependent on the carrier material, operating and curing temperatures, and the maximum strain to be measured [3]. Some

commonly used bonding agents (adhesives) are methyl-2-cyanoacrylate, epoxy, and ceramic-based adhesives [13].

A fairly liberal layer of the adhesive (light but sufficient) was spread on the backs of the gauges and the prepared surfaces. With the aid of the marked axes of the gauges, they were aligned with pre-drawn axes on the test piece so that they were accurately aligned with the axes on the test piece and were set in place at once [3]. A firm but gentle force was applied to push out extra adhesive from under the gauges so that the gauges made just the right contact with the test parts with minimal but sufficient amount of adhesive [3]. It was not necessary to squeeze out all the excess adhesive since this was taken care of by the clamping force that was applied to the gauges while they were being cured or dried [3].

The force applied for curing/drying should be adequate enough for the purpose. Excessive pressures may result in grounding of the gauge wire or lead to the underlying material. For gauges mounted in situations where it is impossible to use a weight, some form of a spring clamp, G or F-clamp etc. may be used [3]. It is good practice to ensure that the material in contact with the strain gauge during drying/curing makes an even/smooth contact with the strain gauge. This would ensure even distribution of the force for curing/drying.

The curing time allowed for a cemented strain gauge partly depends on the type of the adhesive used, upon experience and judgment, and the degree of stability required for the gauge, etc. A minimum of 6 hours was used in this case.

This time also varies somewhat with the gauge construction, the temperature, and humidity of the surrounding environment [3].

The gauges were left to air-dry after curing was completed before lead wires are soldered, if they are so constructed. Allowing the strain gauges to dry adequately ensured that the gauge resistances attained their nominal value [3].

It is also a good and useful practice to adhere to the procedures for bonding and curing the gauge as specified by the gauge manufacturer in their data sheet.

Great care was exercised in soldering the lead wires to the gauges' terminals. It helps in reducing errors if a minimal but adequate amount of solder is used. It is very important to ensure that initial strains are not introduced in the gauge during the early stages, especially when soldering lead wires to the gauge's terminals [3]. It is a common practice to make small loops in the lead wires when soldering them. Pieces of tape were placed on the test surfaces immediately adjacent to the gauges. The soldered lead joints were then held down at those points. These act as shock absorbers for the strain gauge leads and may often prevent an accidentally shorted gauge circuit as well as eliminate external strains on the gauge [3]. All lead wires from the bridge (electrical circuit) to the strain gauge were securely taped to the structure bearing the gauges so that no relative motion occurs.

The gauge resistances were measured after all installation steps were completed. The measured value should be as close as possible to the nominal value quoted by the manufacturer of the gauge. A resistance value that is too low or high most likely indicates

damage to the gauge during the installation stages and the gauge may not be used further. Next, the resistances between the strain gauges' filaments and the test surface to which they are bonded were measured. A thoroughly dried or cured gauge should indicate a resistance in the mega ohms range [3].

A strain gauge cannot in principle perform better than the bond by which it is attached to the test piece [3]. It is therefore apparent that if precise measurement of surface strain is required of the gauge, then the sensitive wire in the strain gauge must have these strains transferred to it by the bonding element. This would only be accomplished by a proper bonding job. In other words, errors introduced by the bonding procedure must be minimized.

The principal characteristics of the cements used for bonding strain gauges must be thoroughly considered for any application because of their potential effects [3].

4.2.2 Bonding Thermocouples

The thermocouples were bonded to their pre-prepared spots in a similar manner as the gauges except that no bonding cement is used with them. Thermocouples were securely held in place with tapes and five-minute epoxy. The spots for the thermocouples were prepared to ensure good thermal contacts with the thermocouples.

4.3 Experimental Procedure

The experimental procedure for acquiring data consists of the gauges and thermocouples bonded on the steel test piece (of sufficient thermal mass) and connected through the RJ 50 cables and NI 9945 modules to the NI 9237 and NI 9211 modules securely placed in slots on the NI cRIO-9012 device. NI LabVIEW 2010 software development suite available on a computer with software variables like resistance of gauges, Poisson's ratio, and bridge configuration set appropriately was used. The NI cRIO-9012 hardware device and external power supply to gauges was provided by an Agilent DC power supply.

Fig.6. Steel test sample (with all sensors bonded)

Fig. 7. NI cRIO-9012 (with NI 9237 and 9211 modules)

Image Credit: Dean K. McNeill

With sensors bonded carefully on the test piece, and with the aid of the hardware and software components, data are acquired at various temperatures. Data acquired corresponds to three experimental scenarios:

- Instrument and test sample in environmental chamber;
- Instrument in and sample out of chamber;
- Instrument out of and sample in chamber.

The environmental chamber was programmed to cycle from –20°C to +20°C in steps of 5°C. Depending on the experimental scenario, the object in the chamber undergoes the cycle above. In some of the experimental scenarios, the temperature indicated by the thermocouples was not the true temperature of the object in the chamber. In these situations, adjusted temperatures are used in the plot of temperature against strain to reflect the temperature cycle of the object in the chamber.

For the first round of tests, strains were acquired before and after switch on of external excitation (9V) by always performing shunt calibration (zeroing of gauges) for all individual temperature steps from –20°C to +20°C.

To observe the effects of the excitation voltage at a given temperature, strains were recorded before and after the switch on of the excitation voltage. It is informative to recall that the test piece is not stressed mechanically in all experimental conditions encountered in this work. As a result, the strains read are mainly apparent strains.

At the point of switch on of the excitation voltage, the strains can be seen to peak as depicted by some of the following sections.

4.4 Data Analysis for First Round of Tests

The data obtained for the first round of tests are presented and analyzed in some sections that follow.

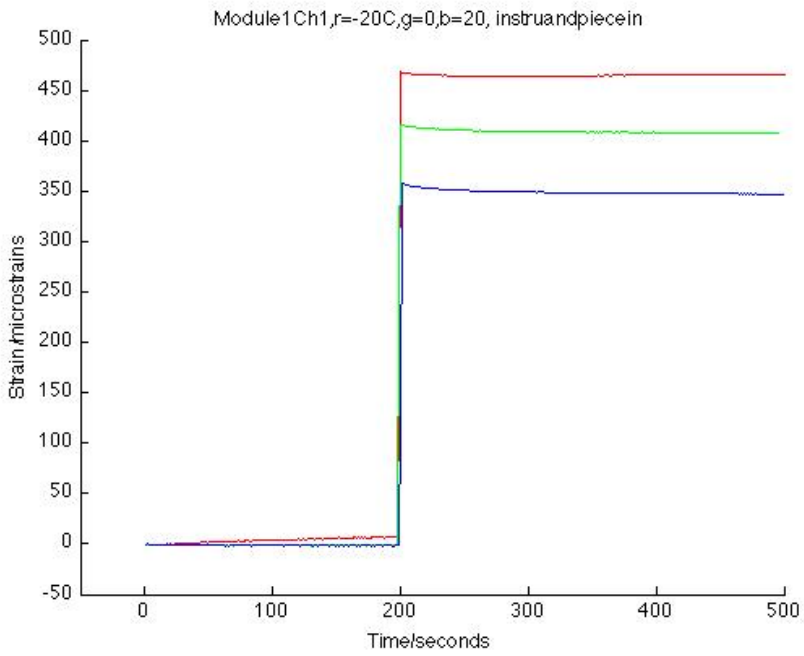

Fig. 8. Plot of thermal output at -20,0 and 20°C against time for channel 1 of module 1

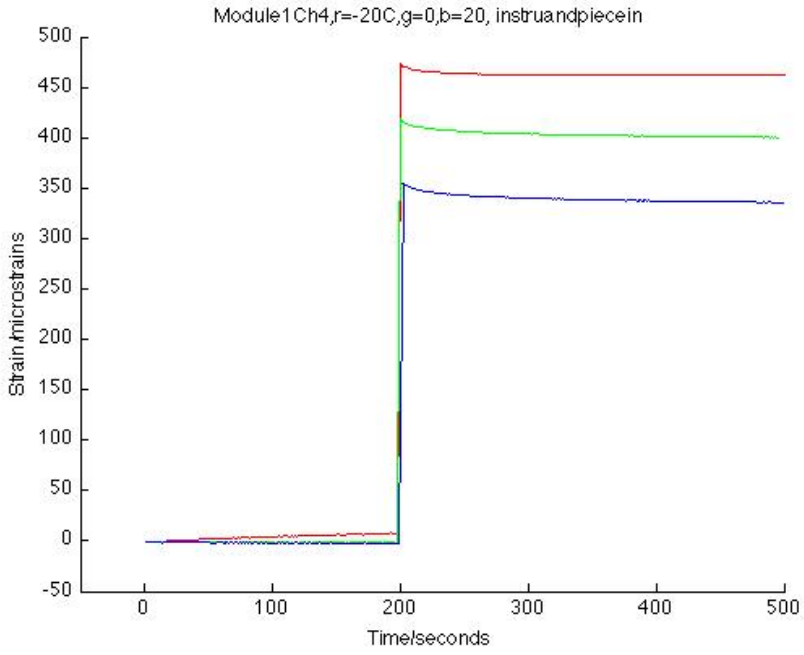

Fig. 9. Plot of thermal output at –20,0 and 20°C against time for channel 4 of module 1

The plots of Fig. 8 and Fig. 9 indicate that there is an instantaneous surge in thermal output upon the instantaneous supply of the external excitation. This is clearly a source of error and hence is undesirable.

Plots exemplifying (highlighting) apparent strains during switch on of the excitation voltage are shown in the following figures.

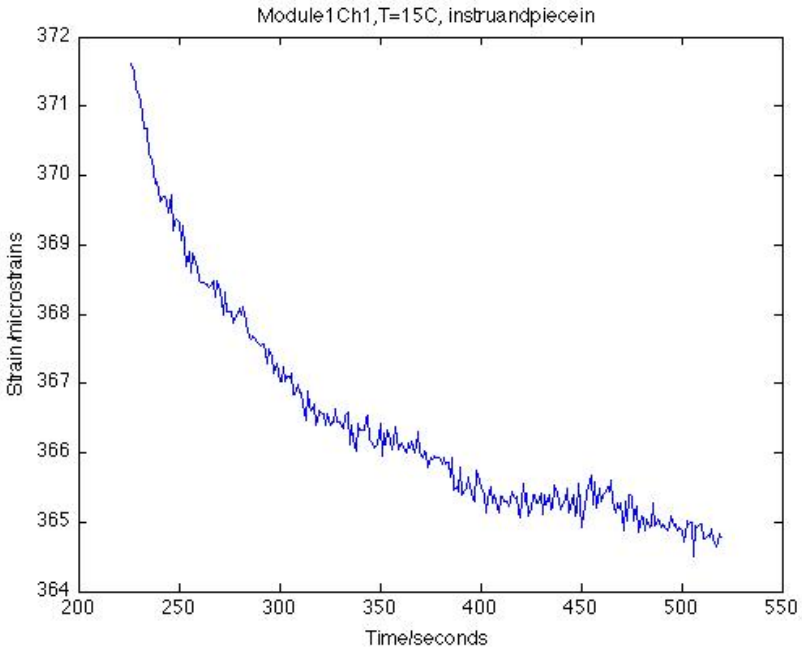

Fig. 10. Plot of thermal output at 15°C against time for channel 1 of module 1

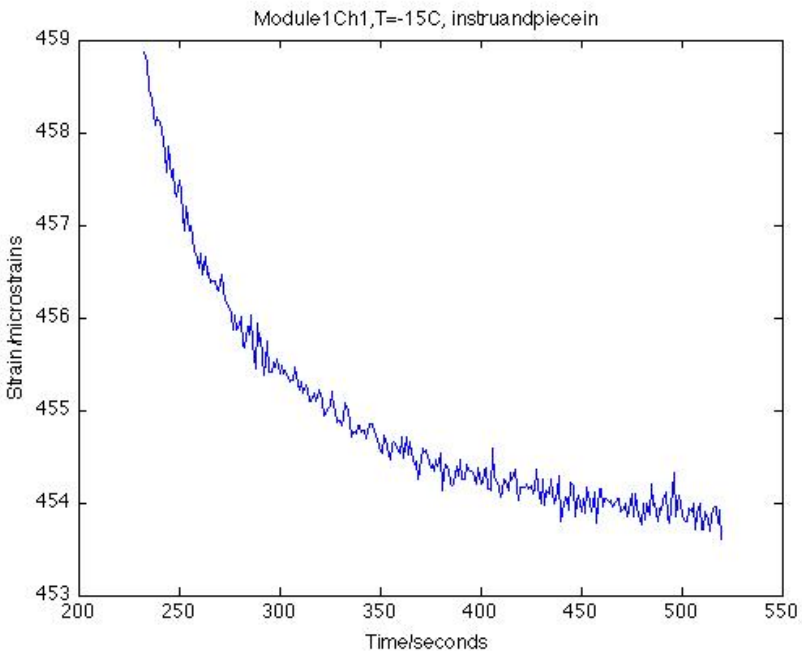

Fig. 11. Plot of thermal output at –15°C against time for channel 1 of module 1

It is seen that after the first peaking of the apparent strains at the point of switch on of the external excitation, they start decaying and settling out somewhat exponentially. It is also seen that the thermal outputs can be minimized if they are allowed to settle upon switch on of the external voltage. Plots of Fig. 10 and Fig. 11 exemplify this.

Various operations like taking strain differences and averaging over strains were carried out to help characterize the effects of the excitation voltage and the temperature variations. Some of these plots are shown below.

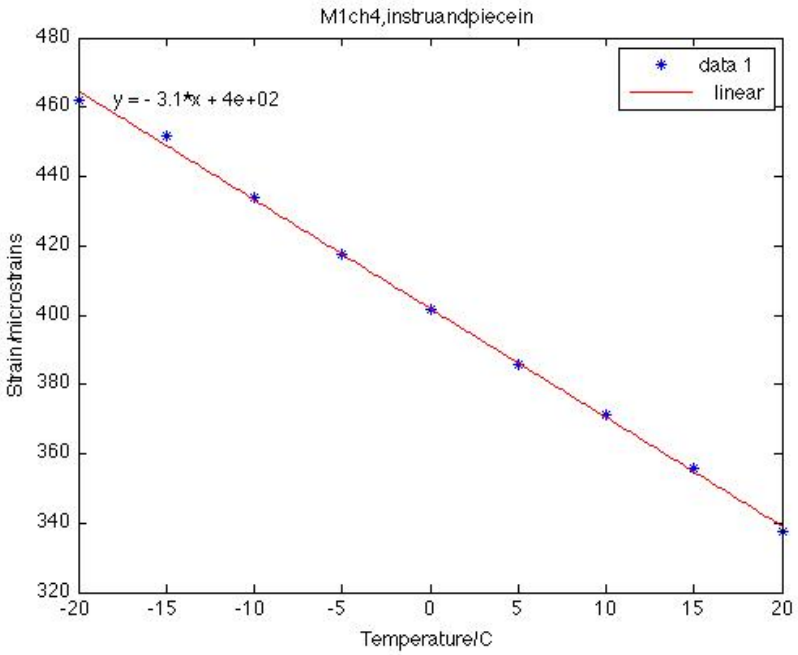

Fig. 12. Plot of thermal output against temperature for channel 4 of module 1

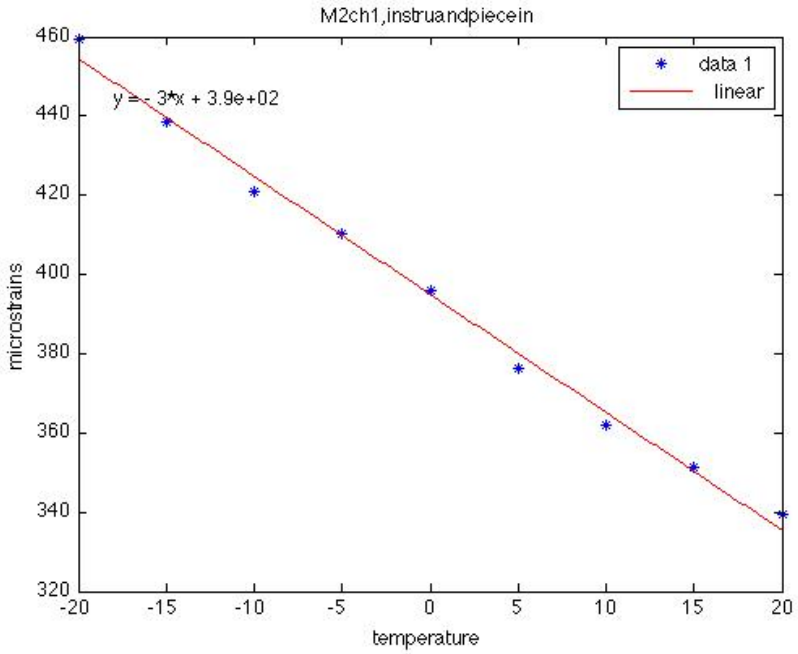

Fig. 13. Plot of thermal output against temperature for channel 1 of module 2

The plots above show data points of the thermal output at the external excitation voltage of 9V(DC) fitted with least squares predictors, as subsequently discussed. The thermal outputs in those plots are taken at a time (e.g. from the 400th second in figures 8 and 9) at which they would have settled somewhat. The least squares approach used for obtaining coefficients for the predictors is outlined below.

The models are developed as follows. Let

$$Y = mT + b \tag{4.1}$$

It follows that the criterion to be minimized is:

$$\Delta^2 = \sum_n \left(y_n - mT_n - b\right)^2.$$

The values of *m* and *b* that minimize the above criterion are obtained from

$$\frac{\partial \Delta^2}{\partial m} = -2\sum_n \left(y_n - mT_n - b\right)T_n = 0 \tag{4.2}$$

$$\frac{\partial \Delta^2}{\partial b} = -2\sum_n \left(y_n - mT_n - b\right) = 0 \tag{4.3}$$

Solving equations 4.2 and 4.3 yields

$$m = \frac{\sum_n T_n \sum_n y_n - N\sum_n T_n y_n}{\left(\sum_n T_n\right)^2 - N\sum_n T_n^2} \tag{4.4}$$

$$b = \frac{\sum_n T_n \sum_n T_n y_n - \sum_n T_n^2 \sum_n y_n}{\left(\sum_n T_n\right)^2 - N\sum_n T_n^2} = \frac{\sum_n y_n - m\sum_n T_n}{N} \tag{4.5}$$

N and *n* are the total number of data points and the nth data point respectively.

These data points fit well in linear predictors with correlation coefficients in –0.90 to

–0.99 range, hence such predictors can be used to determine the thermal output where those conditions pertain (see Fig. 12 and Fig. 13).

To gain insight about the thermal output contribution due to the instrument, the thermal output for the case of the sample out of the chamber and instrument in, is subtracted from the thermal output due to instrument and sample both in the chamber.

Least squares predictors as discussed already were then fitted to the resulting thermal output. The correlation coefficients of the fits ranged from –0.80 to –0.90 Plots oselected results are shown below.

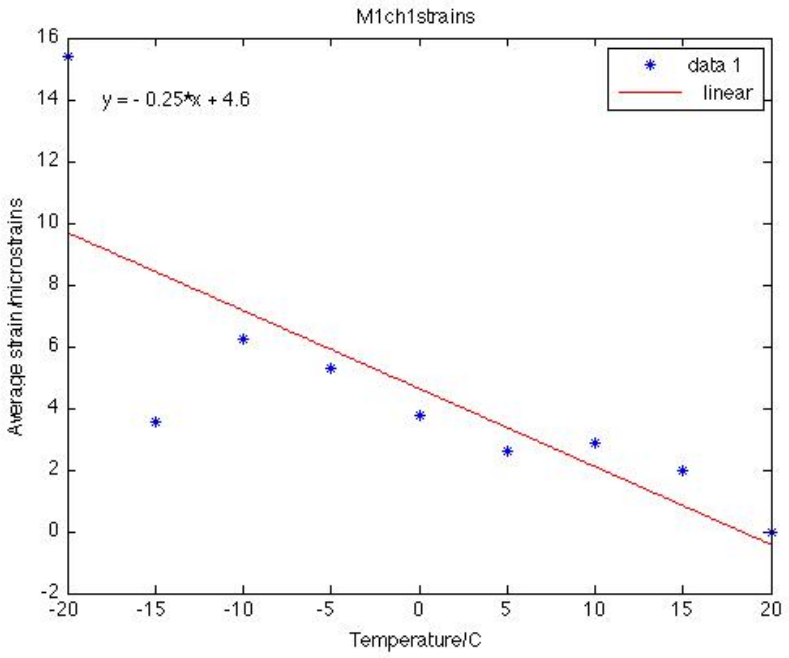

Fig. 14. Plot of compensated thermal output against temperature for channel 1 of module 1

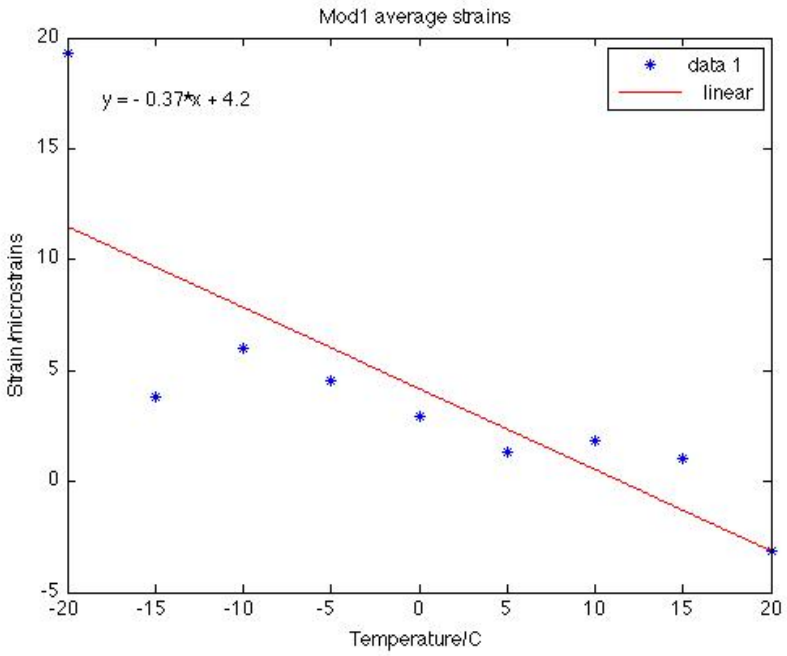

Fig. 15. Plot of compensated thermal output against temperature across all channels of module 1

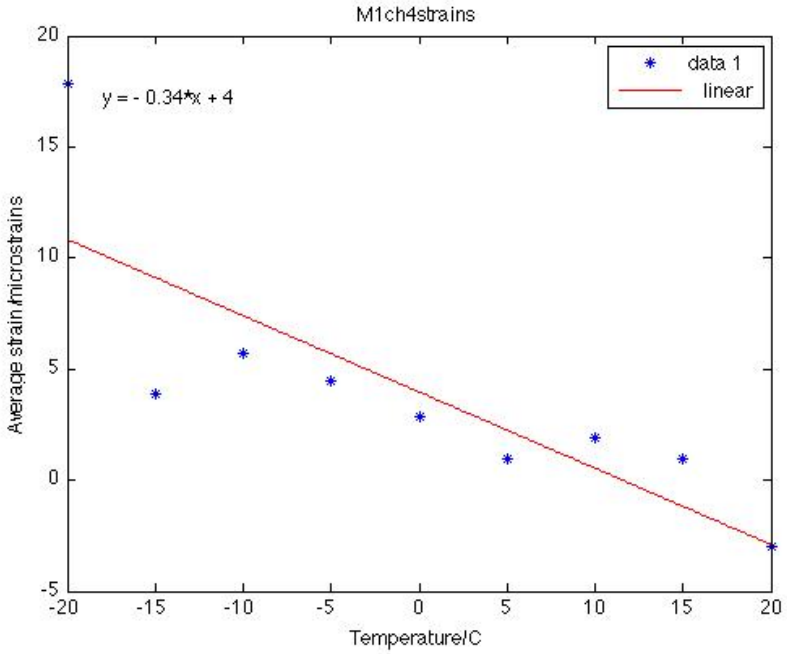

Fig. 16. Plot of compensated thermal output against temperature for channel 4 of module 1

From the analyses of the data from the first round of tests, it is observed that the majority of the apparent strain is attributable to the instrument. Since the gauges are self-temperature-compensated, there is a temperature dependence, but this is on the order of only 5-10με over 40°C (see Figs. 14, 15 and 16).

4.5 Data Analysis for Second Round of Tests

For the second round of tests, data was obtained for the three experimental scenarios using the options available for internal excitation provided by the instrument. Shunt calibration was performed only once, at the beginning of the data acquisition. Also the same temperature range was used but with continuous data acquisition.

4.5.1 Model Development

Models for characterizing the thermal output at the given excitation voltages are developed below. The models are developed for the three experimental scenarios.

4.5.2 Thermal Output Models for Instrument and Steel Test Piece in Chamber

In this scenario, the instrument and the test piece are subjected to the same temperature cycles. The plots of data in this scenario are modeled with least squares fit polynomials.

Let the polynomials to be fitted be represented by

$$Y = aT^i + bT^{i-1} + ... + cT + k$$

Based on the least squares approach, the criterion to be minimized is

$$\Delta^2 = \sum_n \left(y_n - aT_n^i - bT_n^{i-1} - ..... - cT_n - k \right)^2$$

The minimization of the criterion function is achieved by evaluating the partial derivatives of Δ^2 with respect to *a*, *b*, …, *c* and *k* respectively.

That is,

$$\frac{\partial \Delta^2}{\partial a} = -2\sum_n \left(y_n - aT_n^i - bT_n^{i-1} - ... - cT_n - k \right) T_n^i = 0 \tag{4.6}$$

$$\frac{\partial \Delta^2}{\partial b} = -2\sum_n \left(y_n - aT_n^i - bT_n^{i-1} - ... - cT_n - k \right) T_n^{i-1} = 0 \tag{4.7}$$

$$\frac{\partial \Delta^2}{\partial c} = -2\sum_n \left(y_n - aT_n^i - bT_n^{i-1} - ... - cT_n - k \right) T_n = 0 \tag{4.8}$$

$$\frac{\partial \Delta^2}{\partial k} = -2\sum_k \left(y_n - aT_n^i - bT_n^{i-1} - ... - cT_n - k \right) = 0 \tag{4.9}$$

With equal number of equations and of unknowns, the equations are solved to obtain *a*, *b*, …, *c* and *k*.

Plots of data and coefficients of models developed for *i*=3 (i.e. aT^3+bT^2+cT+k) and norms of residuals are shown in the subsequent figures and tables. Coefficients and norms of residuals are given in a clockwise fashion, starting with the topmost left plot. This applies for all data presented henceforth.

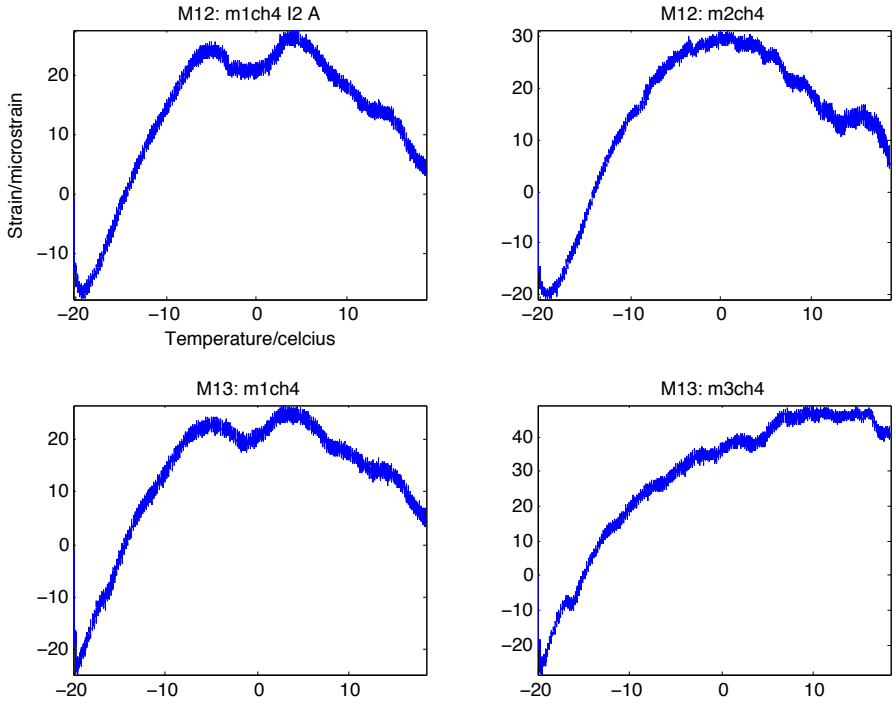

Fig. 17. Plot of temperature against strain for indicated channels in test runs of modules 1 and 2 together and modules 1 and 3 together at 2.5V excitation

Table 2. Coefficients and norm of residuals for polynomials fitted to data in Fig. 17

a	b	c	k	Norm of residuals
0.00098983	-0.084528	0.16017	24.71	386.48
0.0016682	-0.096609	0.12904	27.63	462.59
0.0014502	-0.08467	0.09725	23.84	383.16
0.0011265	-0.071246	1.2312	38.27	414.53

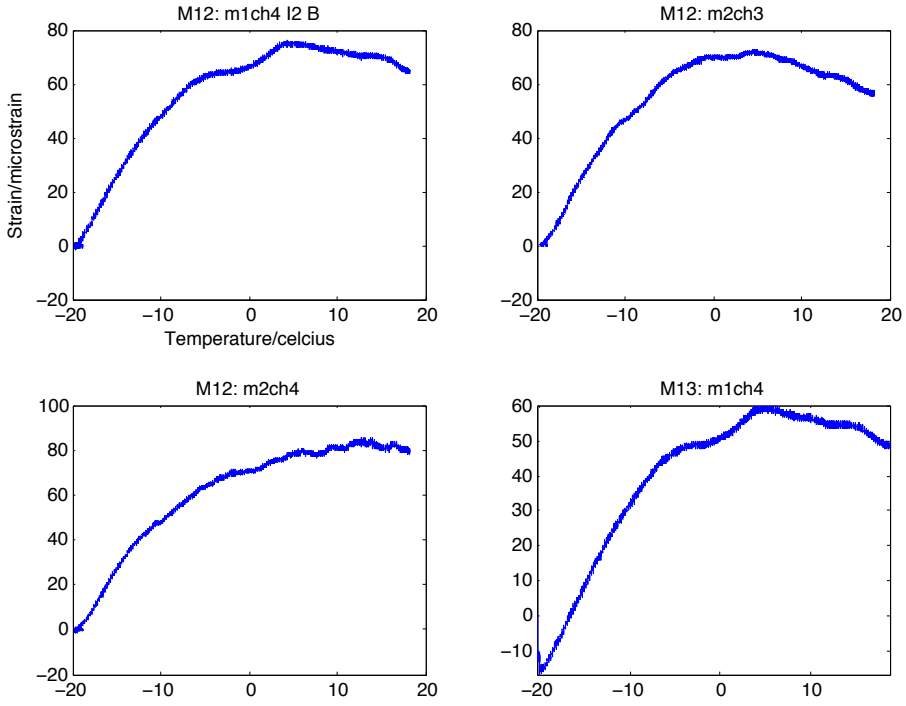

Fig. 18 Plot of temperature against strain for indicated channels in test runs of modules 1 and 2 together and modules 1 and 3 together at 3.3V excitation

Table 3. Coefficients and norm of residuals for polynomials fitted to data in Fig. 18

a	b	c	k	Norm of residuals
0.0015137	-0.098869	1.0926	69.63	250.64
0.0013734	-0.11597	0.87414	69.15	188.2
0.0019384	-0.082719	1.4032	72.53	227.93
0.00090947	-0.095858	1.2019	53.48	331.9

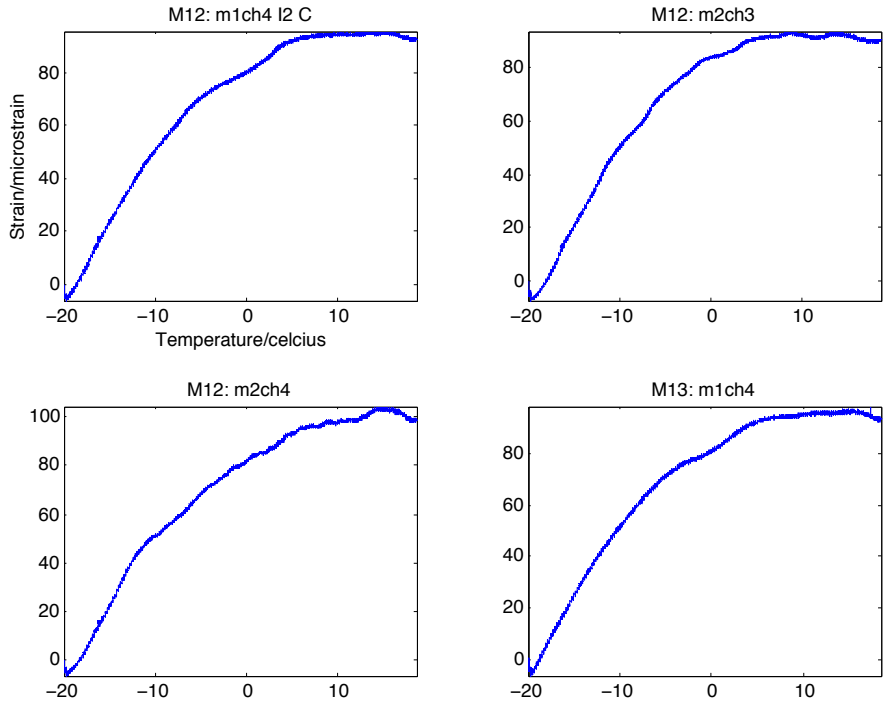

Fig. 19. Plot of temperature against strain for indicated channels in test runs of modules 1 and 2 together and modules 1 and 3 together at 5.0V excitation

Table 4. Coefficients and norm of residuals for polynomials fitted to data in Fig. 19

a	b	c	k	Norm of residuals
0.00083154	-0.10097	2.1317	82.45	212.65
0.00082503	-0.11302	2.1124	82.88	303.46
0.00086242	-0.090575	2.3485	82.73	318.4
0.0010419	-0.10109	2.0951	83.38	185.09

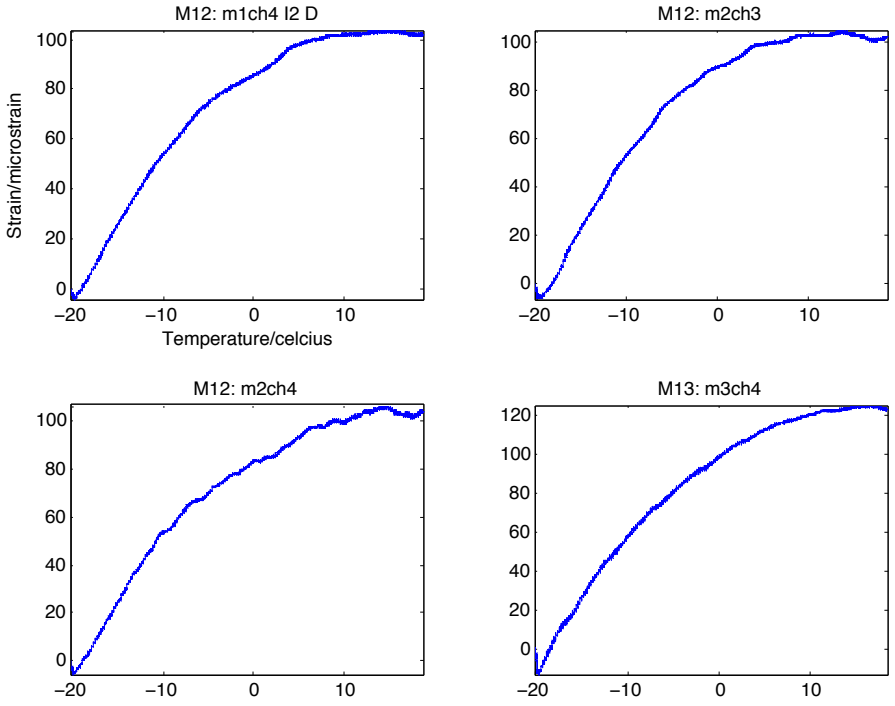

Fig. 20. Plot of temperature against strain for indicated channels in test runs of modules 1 and 2 together and modules 1 and 3 together at 10.0V excitation

Table 5. Coefficients and norm of residuals for polynomials fitted to data in Fig. 20

a	b	c	k	Norm of residuals
0.00069633	-0.10022	2.3728	87.65	210.37
0.00062361	-0.11322	2.4529	89.46	285.05
0.0011118	-0.087131	2.3334	84.18	303.26
0.0006232	-0.10695	3.1064	99.21	253.69

From the coefficients of models fitted to the data in Fig. 17, it is seen that the strains peak to about 25με and then start to decline towards the zero mark. The point at which they

decline to 0με indicates the self-temperature compensation range of the gauges. It is found to be averagely around 24°C for the gauges at excitation of 2.5 V. Also, from the coefficients of the plots for excitations of 3.3,5.0 and 10.0V, we see that after strains peak, they approach the zero mark slowly, as compared to the case of 2.5V. In these situations the thermal output is non-zero at room temperature due to the increased excitations. Evidently, the thermal output is a non-linear function of the temperature.

4.5.3 Thermal Output Models for Instrument in and Steel Piece Out of Chamber

The plots of experimental data in this scenario are fitted with least squares linear predictors. The data acquired in this scenario reflect varying temperature conditions for the instrument but with the sample piece at room temperature through out (approximately 24°C).

Following are plots and tables showing the data and coefficients of fitted regression lines (i.e. Y=mT+b). Model development is discussed in section 4.4.

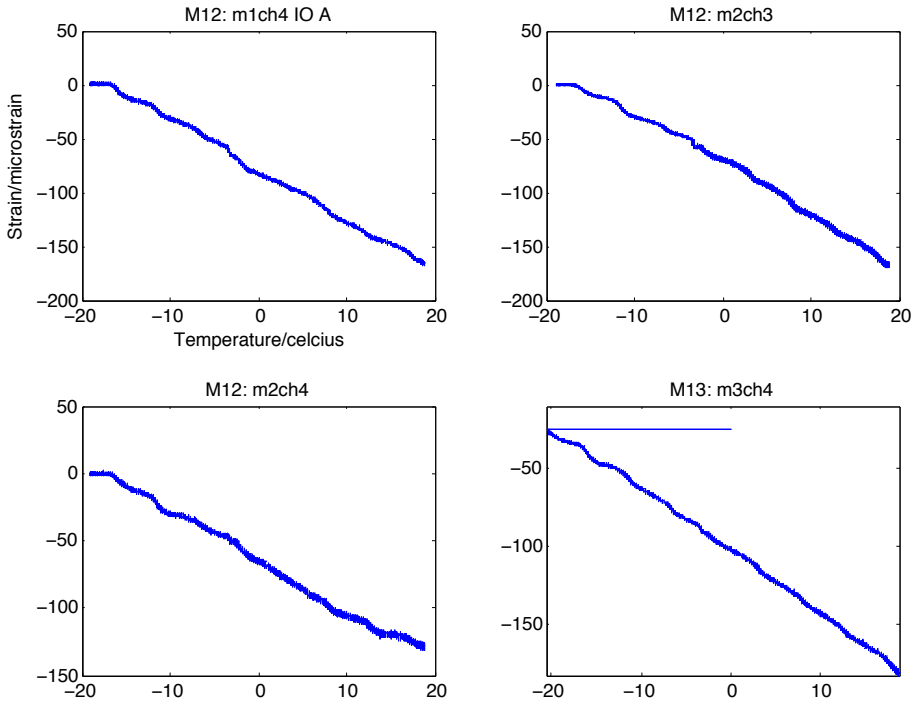

Fig. 21. Plot of temperature against strain for indicated channels in test runs of modules 1 and 2 together and modules 1 and 3 together at 2.5V excitation

Table 6. Coefficients and norm of residuals for polynomials fitted to data in Fig. 21

m	b	Norm of residuals
-4.6696	-79.06	468.99
-4.626	-74.05	730.76
-3.7036	-64.86	531.69
-3.9672	-102.94	313.9

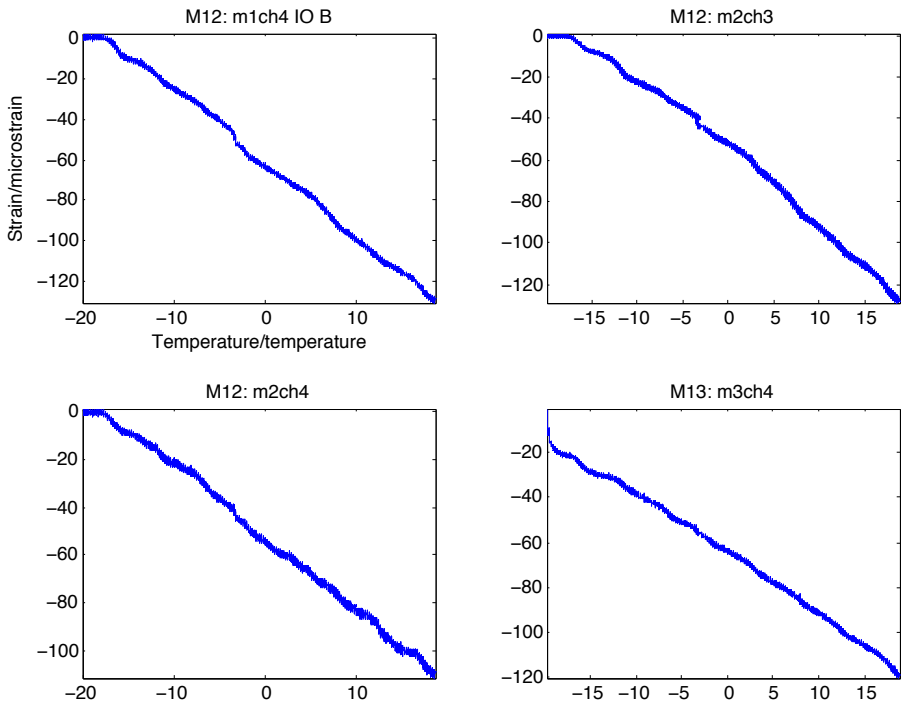

Fig. 22. Plot of temperature against strain for indicated channels in test runs of modules 1 and 2 together and modules 1 and 3 together at 3.3V excitation

Table 7. Coefficients and norm of residuals for polynomials fitted to data in Fig. 22

m	b	Norm of residuals
-3.5542	-62.02	389.15
-3.4695	-56.98	694.73
-2.9828	-53.14	323.02
-2.6513	-65.39	302.94

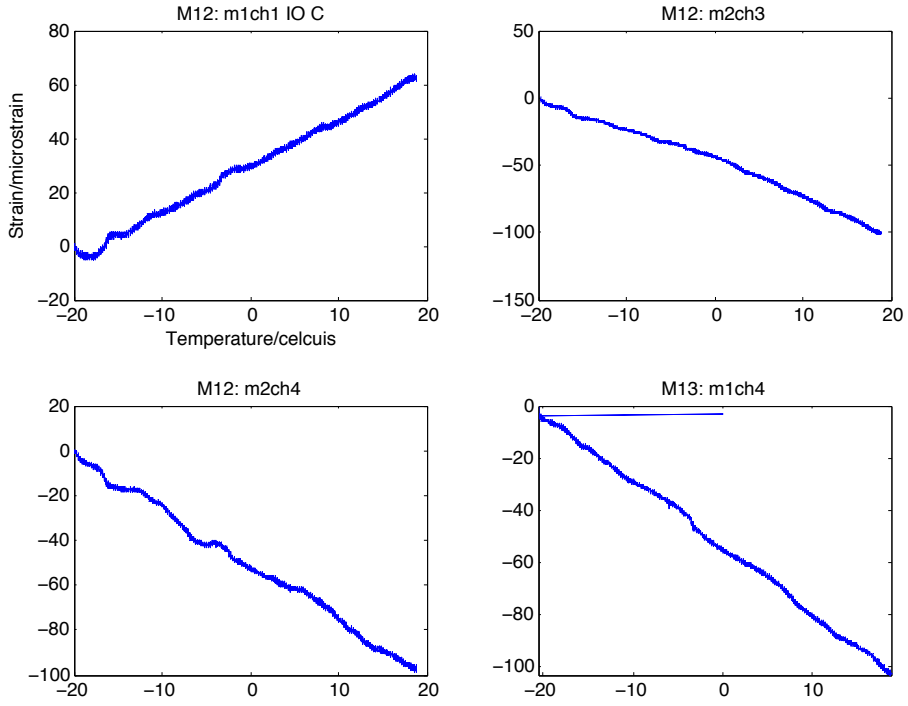

Fig. 23. Plot of temperature against strain for indicated channels in test runs of modules 1 and 2 together and modules 1 and 3 together at 5.0V excitation

Table 8. Coefficients and norm of residuals for polynomials fitted to data in Fig. 23

m	b	Norm of residuals
1.7351	29.62	175.28
-2.5061	-48.69	512.76
-2.4448	-51.39	348.88
-2.5476	-54.00	209.06

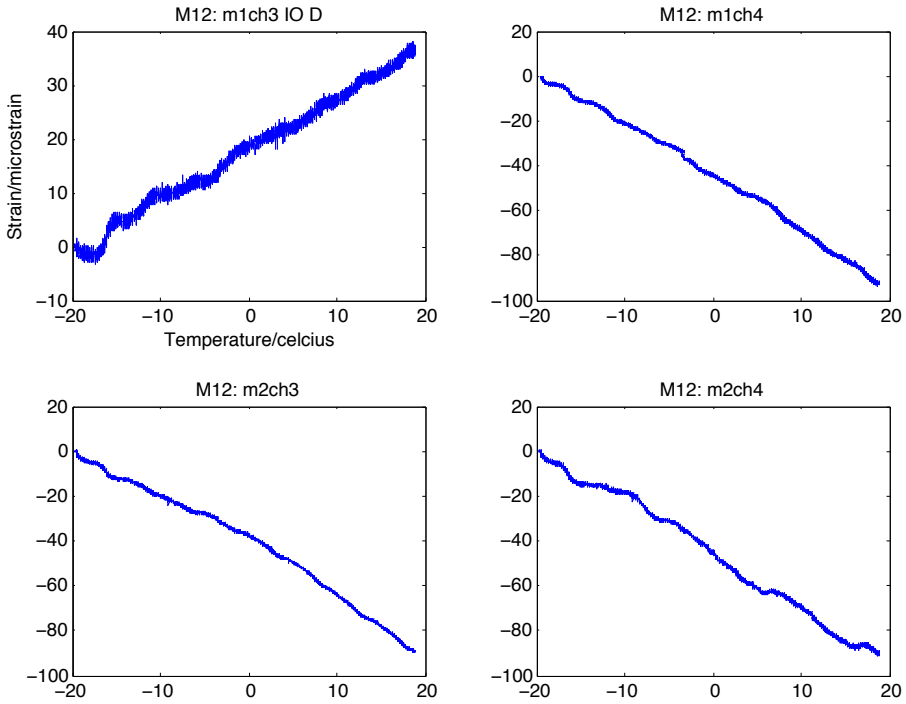

Fig. 24. Plot of temperature against strain for indicated channels in test runs of modules 1 and 2 together at 10.0V excitation

Table 9. Coefficients and norm of residuals for polynomials fitted to data in Fig. 24

m	b	Norm of residuals
0.97375	17.98	175.33
-2.4002	-45.01	286.74
-2.2508	-42.03	519.01
-2.3985	-46.36	432.56

From the plots and models developed, it is seen that strains are in the negative territory. As the excitation voltage increases from 2.5 to 3.3,5.0 and 10.0V, the thermal outputs get increasingly positive for the same temperature points. In these situations, self-temperature

compensation is non-zero at room temperature for all excitations. Strains cross the zero point only at around the -20°C mark, which is not the intended temperature-compensation point. This happened despite the fact that the gauges are compensated for use with the steel test substrate.

The linear predictors sufficiently model the data with correlation coefficients in ±0.95 to ±0.99 range.

4.5.4 Thermal Output Models for Instrument Out and Steel Piece in Chamber

Plots of experimental data in this scenario are also fitted with least squares polynomials. The data obtained for this scenario reflect varying temperature conditions for the steel piece but with the instrument at room temperature through out. The method for determining the coefficients for the polynomials is similar to that in section 4.5.2. Following are plots of the data and tables showing the coefficients and norms of residuals for models fitted to the data for i=3.

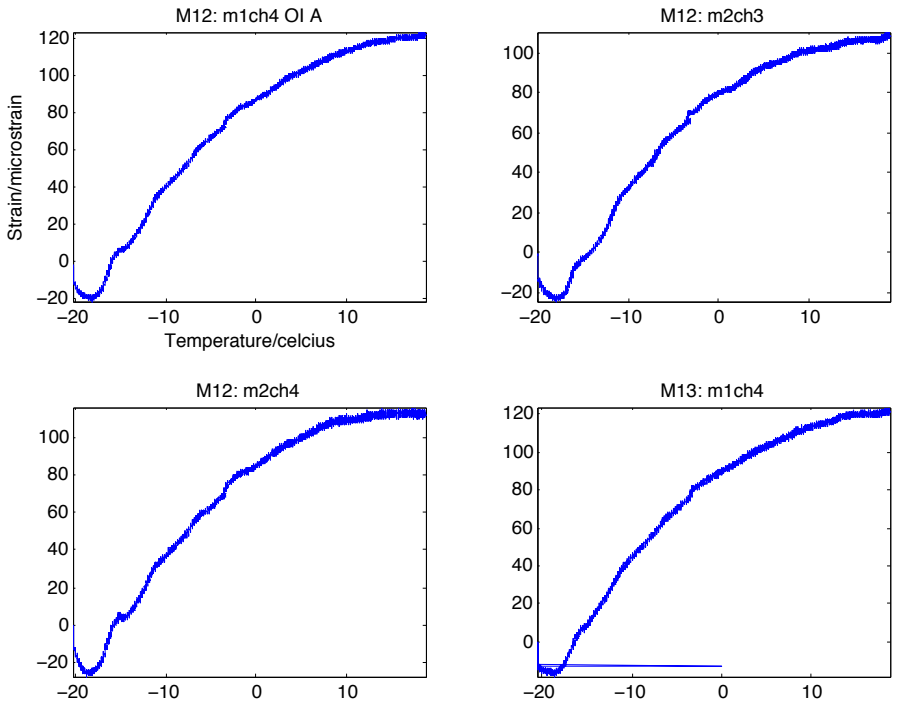

Fig. 25. Plot of temperature against strain for indicated channels in test runs of modules 1 and 2 together and modules 1 and 3 together at 2.5V excitation

Table 10. Coefficients and norm of residuals for polynomials fitted to data in Fig. 25

a	b	c	k	Norm of residuals
-0.00022144	-0.10239	3.7797	86.47	535.35
-0.00051259	-0.10759	3.6501	77.79	670.40
-0.00069094	-0.11512	3.7851	84.59	578.03
-0.000049679	-0.10131	3.5832	88.87	535.02

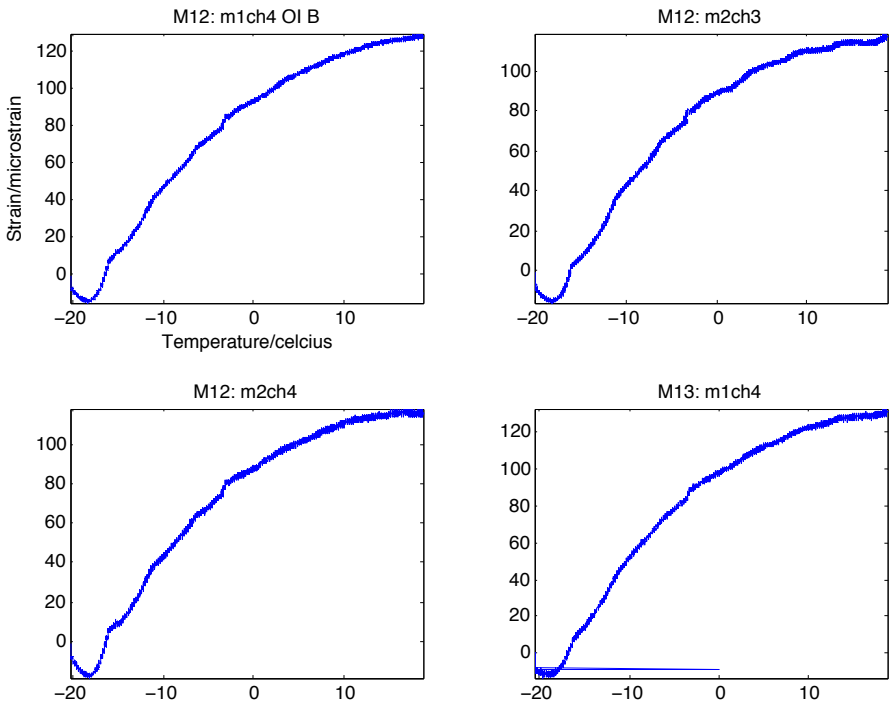

Fig. 26. Plot of temperature against strain for indicated channels in test runs of modules 1 and 2 together and modules 1 and 3 together at 3.3V excitation

Table 11. Coefficients and norm of residuals for polynomials fitted to data in Fig. 26

a	b	c	k	Norm of residuals
0.00017372	-0.10186	3.6655	92.43	509.37
-0.00012981	-0.10991	3.5065	87.25	575.48
0.000069252	-0.10656	3.4383	87.58	550.73
0.000059482	-0.10658	3.6565	97.29	540.51

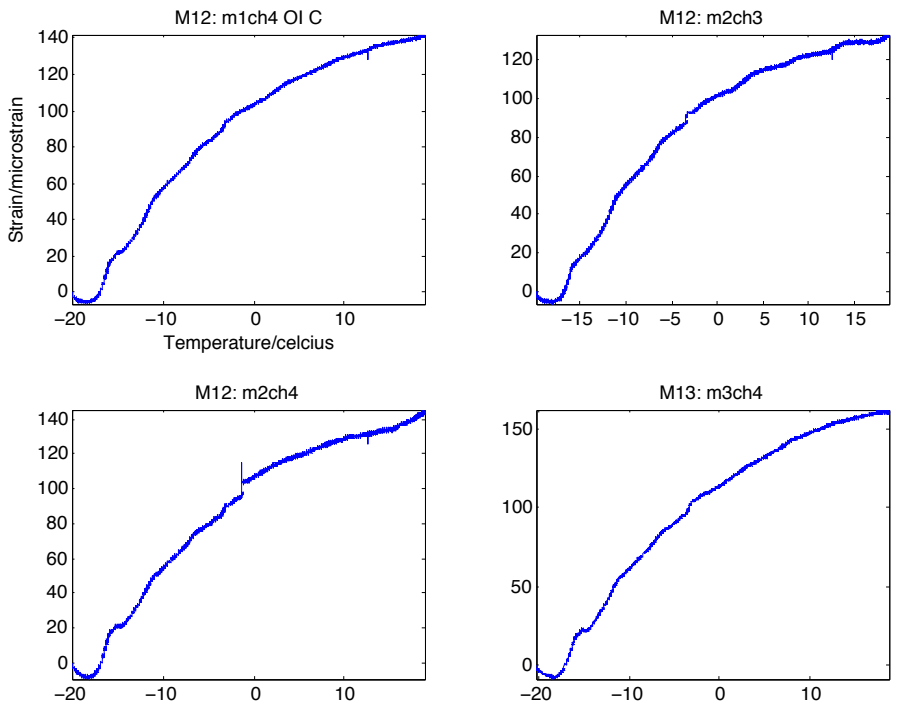

Fig. 27. Plot of temperature against strain for indicated channels in test runs of modules 1 and 2 together and modules 1 and 3 together at 5.0V excitation

Table 12. Coefficients and norm of residuals for polynomials fitted to data in Fig. 27

a	b	c	k	Norm of residuals
0.00076953	-0.10437	3.6515	103.24	448.41
0.00082306	-0.11442	3.4263	100.20	521.90
0.00048203	-0.10488	3.7552	102.46	547.34
0.00015456	-0.10547	4.4109	114.50	518.55

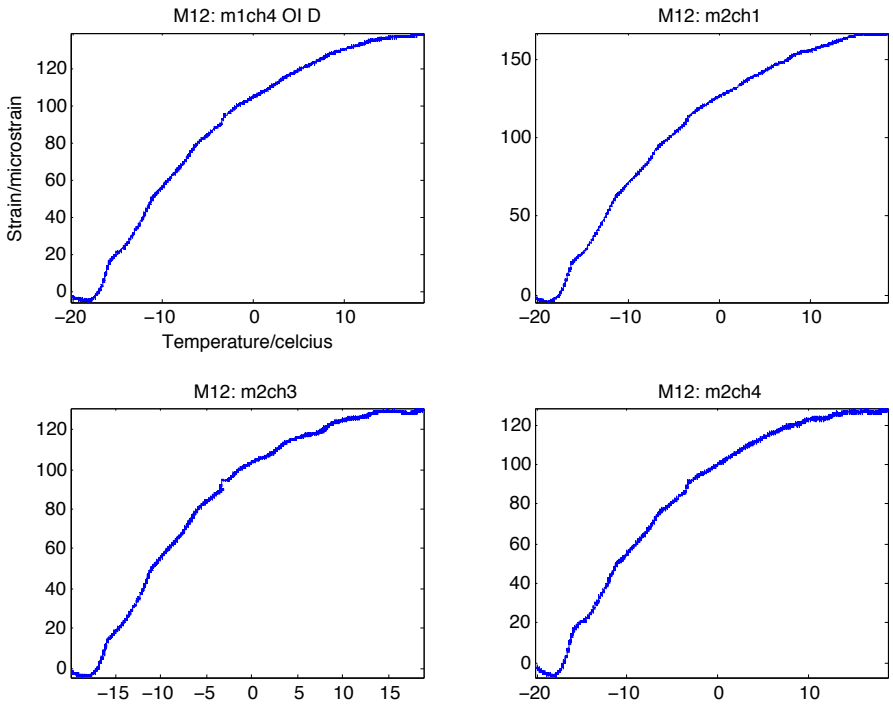

Fig. 28. Plot of temperature against strain for indicated channels in test runs of modules 1 and 2 together at 10.0V excitation

Table 13. Coefficients and norm of residuals for polynomials fitted to data in Fig. 28

a	b	c	k	Norm of residuals
0.00029319	-0.10983	3.7217	104.70	458.79
0.00073998	-0.12804	4.2949	125.98	499.32
0.00034759	-0.11968	3.5009	102.08	512.47
0.00041482	-0.11402	3.3858	99.96	450.60

The data here shows that the thermal output is a non-linear function of temperature. Thermal outputs peak and then start to fall off in all cases. The thermal outputs in these cases are substantially larger than those found in the scenario of instrument and test piece

in the chamber together for the same temperature points and excitations. However, the thermal outputs for higher excitations in this scenario are correspondingly larger than those for lower excitations.

From the plots in the three experimental scenarios above, it is realized that thermal output is substantial although STC gauges are used. The thermal outputs for the scenarios of instrument and test piece together in the chamber and instrument out with test piece in chamber are both nonlinear functions of temperature.

Most of the plots for the case of instrument in with test piece out of the chamber are sufficiently linear with negative slopes. A few plots indicated positive slopes as seen above. This is most likely due to some form of damage to the strain gauges and or the inaccuracies of the internal resistances of the NI 9237 modules to track temperature changes.

Also, the coefficients of all models are in substantial agreement for all the experimental scenarios. Norms of residuals as a measure of performance can aid in model selection.

For the scenario of instrument and test piece in chamber together, at excitation of 2.5V, the STC of the gauges is evident as the temperature approaches room temperature. For higher excitations however, thermal output is non-zero at room temperature because of the increased excitations.

Thermal output data was also obtained using a glass fiber reinforced polymer (GFRP) test piece along the lines of the experimental scenarios discussed already (data not shown

here). These data obtained follow similar trends as those obtained with the steel test piece except that thermal output readings were generally larger than those for the steel test piece for similar temperatures.

Chapter 5

Conclusions, Recommendations and Future Work

5.1 Conclusions and Recommendations

From the models developed, the thermal output is calculated using polynomials of the form $aT^3 + bT^2 + cT + k$ by taking into consideration the experimental scenario and the applicable coefficients.

Thermal outputs for excitation of 2.5V are appreciably lower compared to those of other excitations. Also at this excitation, self-temperature compensation is not destroyed for some situations and should therefore be used where possible. The excitation voltage should be switched on well in advance of the onset of the measurements since their effects would have settled and stabilized.

The thermal output of STC gauges at room temperature may be non-zero depending on the excitation supply, temperature of operation and conditions under which measurements are acquired. These variables should therefore be critically evaluated if self-temperature compensation is to persist.

In order to correct strain measurements for thermal output effects, the thermal output predicted by the appropriate model is subtracted or added to the measurement value, taking into consideration the sign of the thermal output.

The thermal out is substantial for all the experimental scenarios and should therefore be accounted for in measurements in order to obtain reading reflective of a structure's health.

5.2 Future work

The thermal compensation models proposed should be implemented in the software environment so that the resulting strains read are thermally compensated for automatically.

Neural networks solutions for the thermal output problem should be evaluated and compared with the present approach. This would be a basis for the comparability of the methods for the best approach.

References

[1] Dally W.J., Riley F.W., and McConnel G.K., *Instrumentation for Engineering Measurements*, John Wiley & Sons, Inc., 1984,pp.85-202.

[2] Khan S. Akhtar and Wang Xinwei, *Strain Measurements and Stress Analysis*, Prentice Hall, 2001

[3] Perry C.C., and Lissner H.R., *The Strain Gauge Primer*, 1955, McGraw-Hill Book Company, Inc.

[4] Richards L.W., *Strain Gauge Measurement Errors in the Transient Heating of Structural Components*, 1993, NASA Technical Memorandum 104274,p.1

[5] Zhang T., Evans R.G.R., and Rees W.A.D., *The heating effect of electrical resistance strain gauges applied to low thermal conductivity materials*, Strain, August 1992, pp.107-112

[6] Tuttle E.M., and Brinson F.H., *Resistance Foil Strain Gauge Technology as Applied to Composite Materials*, February 1985, NASA Contractor Report 3872

[7] Vishay Micro-Measurements, *Strain Gauge Thermal Output and Gauge Factor Variation with Temperature*, Tech Note TN-504-1, August 2007, pp. 1

[8] Koch J.J., Boiten G.R., Biermasz L.A., Roszbach P.G., and Van Santen W.G., *Strain Gauges Theory and Applications*, 1952

[9] Vishay Micro-Measurements, *Optimizing Strain Gauge Excitation Levels*, Tech Note TN-502, July 2007, pp. 11-17

[10] Hall M.P., and Deighan III A.R., "*On Using Strain gauges in Electronic Assemblies When Temperature is Not Constant*," *IEEE Transactions on Components, Hybrids, and Manufacturing Technology*, Vol. CHMT-9, No.9, 1986, pp.492-497.

[11] Barbosa H.C., Kuhner S.G., Lima A.E., Vellasco M., and Pacheco M., "*Application of a MLP Neural Network for Compensation of Distortions in Strain Gauges Measurements Due to temperature Variations in Offshore Operation of a Flexible Pipe-Lay Vessel*", Proc. Of the International Joint Conference on Neural Networks, 2002,pp. 92-96

[12] Chan C.C., Jin W., Rad B.A., and Demokan S.M., "*Simultaneous Measurement of Temperature and Strain: An Artificial Neural Network Approach*", IEEE Photonics Technology Letters, Vol. 10, No. 6, 1998

[13] ISIS CANADA, *Guidelines for Structural Health Monitoring*, Design Manual No.2, Sept., 2001, pp. A1-A17

[14] Chen G., Deng Y., Sun L., and Xu T., "*A modified Algorithm for Reducing Calculation Errors in Large Strain Measurement with Strain Gauges*", Applied Mechanics and Materials, Vols. 13-14, 2008, pp.261-268